



UNIVERSITÀ DEGLI STUDI DI PADOVA
SCUOLA DI INGEGNERIA
DIPARTIMENTO DI INGEGNERIA DELL'INFORMAZIONE

LAUREA MAGISTRALE IN INGEGNERIA DELL'AUTOMAZIONE

TESI DI LAUREA

**Average Consensus with Prescribed
Performance Guarantees for Multi-agent
Double-Integrator Systems**

Laureando:
Luca MACELLARI

Relatore:
Ch.mo Prof. Alessandro CHIUSO

Relatori presso KTH:
Dr. Yiannis KARAYIANNIDIS
Prof. Dimos V. DIMAROGONAS

10 Marzo 2015

Anno Accademico 2015/2015

Abstract

The problem of consensus reaching with prescribed transient behaviour for a group of agents with dynamics described by a double integrator model is addressed. In order to achieve prescribed performance we employ an appropriately designed transformation of the output error, that reflects performance specifications such as minimum speed of convergence, maximum allowed overshoot and steady state error. Assuming that the information exchange is described by a static communication network, we initially impose time-dependent constraints on the relative positions between neighbouring agents and we design a distributed control law consisting of a proportional term of the transformed error through a transformation related gain and an additional damping term depending on the agent's absolute velocity. Also a second controller is proposed that utilizes the relative velocities between agents that exchange information instead of the absolute velocities. Furthermore, we design a controller that can additionally achieve prescribed performance for the velocity error by imposing time-dependent constraints for a combined error, linear combination of the relative positions and velocities. In this case, the distributed controller has the same structure of the first one enriched with term proportional to the transformed combined error with time variant gains. Under a sufficient condition for the damping gains, the proposed nonlinear time-dependent controllers guarantee that the predefined constraints are not violated and that consensus is achieved with a convergence rate independent of the topology of the communication network. Furthermore, connectivity maintenance can be ensured by appropriately designing the performance bounds. Theoretical results are supported by simulations.

This thesis has been developed at department of Automatic Control, School of Electrical Engineering, KTH – Royal Institute of Technology, Stockholm, during the period September 2014–February 2015. The work has been supervised by Prof. Dimos V. Dimarogonas (Automatic Control, EES, KTH) and Dr. Yiannis Karayiannidis (Centre for Autonomous Systems, KTH)

Contents

Contents	iii
List of Figures	v
List of Symbols	vii
1 Introduction	1
2 Preliminaries and problem formulation	4
2.1 Graph theory	4
2.2 Prescribed performance control	7
2.3 Problem formulation	10
3 Prescribed transient behaviour for the position errors: approach with absolute velocities	12
3.1 Proposed controller	12
3.2 Time evolution of the centroid	13
3.3 Stability analysis	15
3.4 Simulations	17
4 Prescribed transient behaviour for the position errors: approach with relative velocities	22
4.1 Proposed controller	22
4.2 Time evolution of the centroid	23
4.3 Stability analysis	24
4.4 Simulations	29
5 Prescribed transient behaviour for both position errors and combined errors	33
5.1 Combined error	33
5.2 Proposed controller	34
5.3 Time evolution of the centroid	35
5.4 Stability analysis	36
5.5 Simulations	39
6 Conclusions and future work	43
A Derivation of the potential function (3.12) in Theorem 3.1	45

B	Second derivative of the potential function (3.12) in Theorem 3.1	47
C	Derivation of the Lyapunov function (4.20) in Theorem 4.2	50
D	Second derivative of the Lyapunov function (4.20) in Theorem 4.2	51
E	Proof of inequality (5.30)	52
F	Proof of boundedness of $\varepsilon(\hat{q})$ in Theorem 5.1	53
G	Condition (3.11) for an exponentially decreasing performance function	55
H	Proof of inequalities (4.17) and (4.18)	56

List of Figures

2.2	Performance bounds (dashed lines)	7
2.3	Error transformation with natural logarithm.	9
3.1	Communication graph of the multi-agent system used in the simulations: spanning tree \mathcal{G}_1 in solid lines and connected graph with one cycle \mathcal{G}_2 in solid and dashed lines.	18
3.2	Agents trajectories on the x–y plane for PPC1 in case of \mathcal{G}_1 , with $\gamma = 250$ and $G = 36.5I_m$	18
3.3	Relative postitions (solid lines) and performance bounds (dashed lines) in case of \mathcal{G}_1 , with $\gamma = 250$ and $G = 36.5I_m$	19
3.4	Absolute velocities along (a) x coordinate and (b) y coordinate in case of \mathcal{G}_1 , with $\gamma = 250$ and $G = 36.5I_m$	20
3.5	Absolute velocities along the x coordinate with $\gamma = 50$ and $G = 7.8I_m$, in case of \mathcal{G}_1	20
3.6	Response of the total distance from the centroid for PPC1 in the case of \mathcal{G}_1 : confront between $G = I_m$ and $G = 36.5I_m$	20
3.7	Comparison between PPC1 (solid line), with $\gamma = 250$ and $G = 36.5I_m$, and the linear protocol (dashed line). Case of \mathcal{G}_1	21
3.8	Comparison of PPC1 performance depending on the topology of connec- tions between agents. Distance from the centroid. $\gamma = 250$ and $G = 36.5I_m$. 21	21
3.9	Control inputs along (a) x coordinate and (b) y coordinate in case of \mathcal{G}_1 , with $\gamma = 250$ and $G = 36.5I_m$	21
3.10	Relative velocities along (a) x coordinate and (b) y coordinate in case of \mathcal{G}_1 , with $\gamma = 250$ and $G = 36.5I_m$	21
4.1	Agents trajectories on the x – y plane with PPC2 in case of \mathcal{G}_1 . $\gamma = 390$ and $G = 36I_m$	29
4.2	Relative postitions (solid lines) and performance bounds (dashed lines) in case of \mathcal{G}_1 , with $\gamma = 390$ and $G = 36I_m$	30
4.3	Absolute velocities along (a) x coordinate and (b) y coordinate in case of \mathcal{G}_1 , with $\gamma = 390$ and $G = 36I_m$	31
4.4	Relative velocities along (a) x coordinate and (b) y coordinate in case of \mathcal{G}_1 , with $\gamma = 390$ and $G = 36I_m$	31
4.5	Control inputs along (a) x coordinate and (b) y coordinate in case of \mathcal{G}_1 , with $\gamma = 360$ and $G = 36I_m$	31
4.6	Comparison of nonlinear (PPC2, solid line) and linear (dashed line) pro- tocol in case of \mathcal{G}_1 : time evolution of the distance from the centroid. . . .	32
4.7	Comparison of the performance of PPC2 with different topologies for the connections between agents.	32

5.1	Agents trajectories on the $x - y$ plane with PPC3 in case of \mathcal{G}_1 , with $G = 2I_m$, $\gamma = 3$.	39
5.2	Absolute velocities along (a) x coordinate and (b) y coordinate in case of \mathcal{G}_1 , with $\gamma = 3$ and $G = 2I_m$.	40
5.3	Relative velocities along (a) x coordinate and (b) y coordinate in case of \mathcal{G}_1 , with $\gamma = 3$ and $G = 2I_m$.	40
5.4	Comparison between PPC3 (solid line), with $\gamma = 3$ and $G = 2I_m$, and the linear protocol (dashed line). Case of \mathcal{G}_1 .	40
5.5	Comparison of the performance of PPC3 for different graph topologies. Distance from the centroid. $\gamma = 3$, $G = 2I_m$	40
5.6	Control inputs along (a) x coordinate and (b) y coordinate in case of \mathcal{G}_1 , with $\gamma = 3$ and $G = 2I_m$.	41
5.7	Relative positions (solid lines) and performance bounds (dashed lines) in case of \mathcal{G}_1 , with $\gamma = 3$ and $G = 2I_m$.	42
5.8	Combined error (solid lines) and performance bounds (dashed lines) in case of \mathcal{G}_1 , with $\gamma = 3$ and $G = 2I_m$.	42

List of Symbols

$ \cdot $	Absolute value of a real number or cardinality of a set
$\ \cdot\ $	Euclidean norm of a vector or a matrix
I_n	Identity matrix of dimension n
$\mathbb{1}_n$	$n \times 1$ vector of all ones
$\mathbf{0}_n$	$n \times 1$ vector of all zeros
\mathcal{G}	Graph of interconnections between agents
\mathcal{V}	Set of vertices of a graph
\mathcal{E}	Set of edges of a graph
N	Number of agents
m	Number of edges
\mathcal{A}	Adjacency matrix of a graph
Δ	Degree matrix of a graph
B	Incidence matrix of a graph
\mathcal{N}_i	Neighbour set of the agent i
L	Laplacian matrix of a graph
L_E	Edge Laplacian matrix of a graph
$\lambda_{\min}(\cdot)$	Minimum eigenvalue of a matrix
$\lambda_{\max}(\cdot)$	Maximum eigenvalue of a matrix
$\lambda_i(\cdot)$	i -th eigenvalue of a matrix
x_i	Position of agent i
v_i	Velocity of agent i
x_{ij}	Relative position (or position error) between agent i and j
v_{ij}	Relative velocity (or velocity error) between agent i and j
q_{ij}	Combined error between agent i and j
\bar{x}_k	Position error (or relative position) between the agents connected by the k -th edge
\bar{v}_k	Velocity error (or relative velocity) between the agents connected by the k -th edge
\bar{q}_k	Combined error between the agents connected by the k -th edge

\hat{x}_{ij}	Modified relative position between agent i and j
\hat{x}_k	Modified position error between the agents connected by the k -th edge
\hat{q}_k	Modified combined error between the agents connected by the k -th edge
ξ	State vector of the multi-agent system
ξ^*	Equilibrium of the multi-agent system
e	Distance from the equilibrium point
\mathbf{e}	Disagreement vector
$\varepsilon_{ij}(\cdot)$	Transformed error between agents i and j
$\varepsilon_k(\cdot)$	Transformed error between agents connected by the k -th edge
\bar{x}	Stack vector of position errors
\bar{v}	Stack vector of velocity errors
\bar{q}	Stack vector of combined errors
$\hat{\bar{x}}$	Stack vector of modified position errors
$\hat{\bar{q}}$	Stack vector of modified combined errors
$\varepsilon(\cdot)$	Stack vector of transformed errors
$\rho_{ij}(t)$	Performance function for the error between agents i and j
$\rho_k(t)$	Performance function for the error between agents connected by the k -th edge
$T_{ij}(\cdot)$	Transformation function for the error between agents i and j
$T_k(\cdot)$	Transformation function for the error between agents connected by the k -th edge
M_{ij}	Overshoot index for the error between agents i and j
$\alpha_{ij}(t)$	Normalized derivative of $\rho_{ij}(t)$
$\alpha_k(t)$	Normalized derivative of $\rho_k(t)$
$\mathcal{J}_{T_{ij}}(\cdot, t)$	Normalized jacobian of the transformation function T_{ij}
$\mathcal{J}_T(\cdot, t)$	Diagonal matrix with elements $\mathcal{J}_{T_{ij}}(\cdot, t)$
$P(t)$	Diagonal matrix with elements $\rho_{ij}(t)$ (or $\rho_k(t)$)
$A(t)$	Diagonal matrix with elements $\alpha_{ij}(t)$ (or $\alpha_k(t)$)
$c(t)$	Centroid of the multi-agent system
c_∞	Final value of the centroid of the multi-agent system
g_{ij}	Constant gain
G	Diagonal gain matrix with elements g_{ij}
γ	Damping gain of the nonlinear consensus protocol
p	Position of an agent on the $x - y$ plane
γ_L	Damping gain of the linear consensus protocol
Γ_L	State matrix of the linear consensus protocol

Chapter 1

Introduction

Distributed control of multi-agent systems is a relatively recent research area that is of great interest due to the large variety of applications. A multi-agent system consists of a collection of dynamical systems, called agents, that are able to exchange information over a communication network. Cooperative control and formation control of unmanned aerial vehicles and wheeled vehicles as well as energy systems, sensor networks, security camera networks are only a few examples of the diverse fields in which this kind of systems can be exploited. Some tasks such as patrolling, exploration and surveillance can be carried out by a single autonomous agent, but having at disposal multiple agents able to interact and cooperate allows to perform these tasks more efficiently and on a larger scale. A centralized approach to the control of a group of agents would require a considerable computational effort, growing with the number of agents, and would not ensure robustness to system failures. To overcome these drawbacks, distributed control algorithms based on local information exchange are applied: each agent updates its current state evaluating only the states of the agents it can communicate with. However, this type of approach introduces a new set of problems and challenges that need to be taken into account and require specific mathematical tools.

When dealing with a group of agents the control objectives can be various, ranging from agreement on a measured value, in the case of sensor networks, to rendez-vous [1] (agreement on position), flocking [2] or platooning [3], in the case of multiple vehicles. The problem of ensuring convergence to the same value is commonly known as consensus: one of the first theoretical frameworks to address this problem was given by Olfati-Saber et al. [4,5]. A typical approach to consensus consists in describing the way agents exchange information with a graph, in which each vertex represents an agent and the edges represent the communication links. A communication network in which some agents are only able to receive information and others can only transmit can be

modelled with directed graphs [6], whereas if the agents have the same capabilities and the exchange is bidirectional undirected graphs are used [7]. In this framework, the properties of the multi-agent system are strictly related to the algebraic properties of the graph matrices and the results of algebraic graph theory can be exploited to determine the behaviour of the system. In particular, for many linear agreement protocols the conditions guaranteeing convergence, and the rate of convergence, depend on the eigenvalues of the Laplacian matrix [8], [9]. Since the agents are moving during time, their relative positions change and some links can fail as well as new one can be created due to communication constraints: this situation can be described with time-variant graphs. In [10] the problem of consensus seeking for first-order and second-order agents under switching topology is treated and it is shown that convergence properties depend on the second smallest eigenvalue of the Laplacian. It is important to notice that the fundamental assumption that characterizes all the mentioned works is the connectedness of the underlying communication graph. Lack of connectedness, in fact, implies that one or more agents are not exchanging any information, therefore they are not able to reach a common value with the rest of the group. Various solutions have been proposed for the issue of connectivity maintenance. For example, in [11] constraints in the edge's space are imposed, introducing potential functions which value goes to infinity when approaching the critical distance between two agents. It also is shown that if the initial conditions are confined within a certain region, consensus is achieved while preserving connectedness.

In general, constraints in the evolution of the state or the output of both linear and nonlinear systems have been handled with a variety of different control techniques (e.g. model predictive control [12], logarithmic barrier Lyapunov functions [13], prescribed performance control [14], funnel control [15]). Prescribed performance control has been formalized by Bechioulis and Rovithakis in [16], [17] and it has been applied to feedback linearizable and strict feedback nonlinear systems to solve the tracking problem. A prescribed performance controller ensures that the tracking error converges to an arbitrarily small residual set, with a rate not less than a given value and with an overshoot less than a specified value. To achieve this the tracking error is transformed with a function, similar to a barrier function, which goes to infinity while approaching the predefined bounds. Recently these controllers have been successfully applied to manipulators and robots: for example in [18] a PID controller enriched with a prescribed performance term has been designed to solve the joint position regulation and the tracking problems whereas in [19] unicycle-like robots are considered.

In this work, the framework of prescribed performance control is applied to multi-agent systems. A set of time-dependent constraints are introduced on the edge's space, forcing the errors between communicating agent to evolve within predefined bounds. The objective is to design a distributed law to achieve consensus while ensuring that the relative positions of neighbouring agents evolve without violating the constraints. This approach decouples the convergence rate of the system from the communication graph, allowing to reach consensus in arbitrarily fast time by appropriately designing the performance function. Furthermore, connectivity maintenance during the agent's motion can be ensured by properly defining the bounds. The average consensus problem with prescribed performance guarantees has already been introduced in [20] for first-order integrator agents: along the lines of this paper, we extend the results to second-order integrator multi-agent systems. This extension is of particular interest since a variety of vehicles need a double-integrator model to be described and some vehicle dynamics, e.g. nonholonomic models, can be feedback linearized to a second-order integrator [8]. Three different nonlinear time-dependent agreement protocols are proposed: the first two distributed controllers are designed in order to ensure that the position errors between communicating agents evolve within some predefined bounds whereas the third also guarantees that some additional time-dependent constraints on the relative velocities are satisfied. Under certain assumptions, all the characteristics of the first-order protocol are preserved, including convergence to the invariant centroid. Lyapunov-like methods are used to investigate stability of the closed loop systems and conditions for convergence are derived. The different controllers are simulated considering different topologies for the underlying graph.

The thesis is organized as follows: in Chapter 2 the mathematical tools used throughout the work are introduced and the control objective is plainly stated; in Chapter 3 the first proposed controller is presented, stability and convergence properties are studied and simulations are provided; Chapter 4 and 5 follow the same structure of the previous one presenting the second and the third proposed controllers; Chapter 6 summarizes the results and discusses future developments. Appendices provide the proofs omitted in the previous chapters.

Chapter 2

Preliminaries and problem formulation

2.1 Graph theory

Graphs are a useful tool to model the topology of the connections between agents, in multi-agent systems. In this section we provide a brief overview of the concepts of graph theory that will be widely used throughout the whole thesis. A graph \mathcal{G} with N vertices and m edges is usually characterized with two finite sets: $\mathcal{V} = \{1, 2, \dots, N\}$ is the set of vertices and $\mathcal{E} = \{(i, j) \in \mathcal{V} \times \mathcal{V} | j \in \mathcal{N}_i\}$ is the set of edges and, obviously, N and m are the cardinalities of \mathcal{V} and \mathcal{E} respectively. \mathcal{N}_i is the *neighbourhood* of vertex i , i.e. the set of all the vertices j that are adjacent to i ; two vertices i and j are said to be *adjacent* if there is an edge connecting them. If the communication topology is changing during time, the sets \mathcal{N}_i are time-variant.

A graph is *directed* if the edges are oriented, i.e. the pairs $(i, j) \in \mathcal{E}$ are ordered, otherwise it is *undirected*. A *path* of length r from i to j is a sequence of $r + 1$ distinct vertices starting from i and ending with j , such that consecutive vertices are adjacent. If the starting and ending vertices coincide, then we have a *cycle*. A graph is *connected* if there is a path between any pair of vertices, otherwise it is disconnected. Additionally, a connected graph without cycles is referred to as a *tree*.

To each graph is associated a $N \times N$ matrix, the *adjacency matrix* $\mathcal{A} = \mathcal{A}(\mathcal{G}) = [a_{ij}]$, representing the adjacency relationships between the vertices: each element a_{ij} is equal to 1 if $(i, j) \in \mathcal{E}$ and equal to 0 otherwise. If the graph is undirected \mathcal{A} is symmetric.

We call *degree matrix* $\Delta = \text{diag} \{\delta_1, \delta_2, \dots, \delta_N\}$ the $N \times N$ diagonal matrix containing the degrees of the vertices of the graph: the *degree* of the vertex i is the number of incident edges and it is given by $\delta_i = \sum_{j=1}^N a_{ij}$. By assigning an orientation to each edge

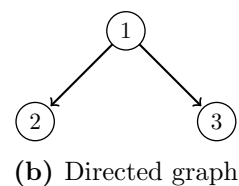
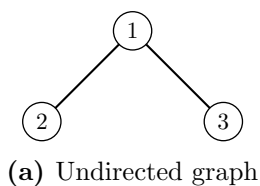
of \mathcal{G} we can define the *incidence* matrix, a $N \times m$ matrix denoted by $B = B(\mathcal{G}) = [b_{ij}]$. The rows of B are indexed by the vertices and the columns are indexed by the edges. In particular $b_{ij} = 1$ if the vertex i is the head of the edge j , $b_{ij} = -1$ if i is the tail of edge j and $b_{ij} = 0$ otherwise. The rank of B and the connectivity properties of the relative graph are strictly related, as Theorem 2.1 in [21] states: for a graph with h connected components, $\text{rank}(B) = N - h$. Another important property of the incidence matrix is that the null space of its transpose, $\text{Ker}(B^\top)$, is spanned by the vector $\mathbb{1}_N = [1, 1, \dots, 1]^\top$. We define the *Laplacian* matrix of \mathcal{G} as $L = \Delta - \mathcal{A}$. We can also obtain the Laplacian matrix as $L = BB^\top$. For an undirected graph L is a rank deficient, symmetric, positive semi-definite matrix, whereas for directed graphs it does not have these properties. In both cases, if the graph is connected, L has a single zero eigenvalue with $\mathbb{1}_N$ corresponding eigenvector [21]. Therefore, the real spectrum of the Laplacian can be ordered as

$$0 = \lambda_1(L) \leq \lambda_2(L) \leq \dots \leq \lambda_N(L)$$

As a consequence of the previously cited theorem (Theorem 2.1, [21]), the multiplicity of the zero eigenvalue of the graph Laplacian is equal to the number of connected components of \mathcal{G} . We define the *edge Laplacian* as $L_E = B^\top B$: it is a $m \times m$ symmetric matrix and it is positive definite if and only if the graph is a tree. The spectral properties of L_E are strictly related to those of L since they have the same non zero eigenvalues [9], [6].

Example 1. Consider a simple undirected graph with $N = 3$ and $m = 2$ with the topology of Figure 2.1a. This is a connected graph, without cycles, therefore it is a tree. Its associated adjacency, degree and Laplacian matrix are, respectively,

$$\mathcal{A} = \begin{bmatrix} 0 & 1 & 1 \\ 1 & 0 & 0 \\ 1 & 0 & 0 \end{bmatrix} \quad \Delta = \begin{bmatrix} 2 & 0 & 0 \\ 0 & 1 & 0 \\ 0 & 0 & 1 \end{bmatrix} \quad L = \begin{bmatrix} 2 & -1 & -1 \\ -1 & 1 & 0 \\ -1 & 0 & 1 \end{bmatrix}$$



Assigning an orientation to the edges (Figure 2.1b) we can define the incidence matrix

$$B = \begin{bmatrix} 1 & 1 \\ -1 & 0 \\ 0 & -1 \end{bmatrix}$$

and easily verify all its properties: the sum of the elements on the columns is equal to zero, equivalently $\mathbb{1}_3^\top B = 0$, and $L = BB^\top$.

The eigenvalues of the Laplacian matrix are $\lambda(L) = \{0, 1, 3\}$ in accordance with the fact that the graph is connected. The edge Laplacian is

$$L_E = \begin{bmatrix} 2 & 1 \\ 1 & 2 \end{bmatrix}$$

and its eigenvalues are $\lambda(L_E) = \{1, 3\}$, verifying the aforementioned relationship between the two Laplacians. \triangle

Before concluding the section, let us cite an important result on the characterization of the eigenvalues of an Hermitian matrix [22]. The theorem is stated below for the specific case of a symmetric matrix :

Theorem (Courant-Fischer). *Let $F \in \mathbb{R}^{n \times n}$ be a symmetric matrix with eigenvalues $\lambda_1(F) \leq \lambda_2(F) \leq \dots \leq \lambda_n(F)$ and let k be an integer with $1 \leq k \leq n$. Then*

$$\min_{w_1, w_2, \dots, w_{n-k} \in \mathbb{R}^n} \max_{\substack{z \neq 0, z \in \mathbb{R}^n \\ z \perp w_1, w_2, \dots, w_{n-k}}} \frac{z^\top F z}{z^\top z} = \lambda_k(F)$$

and

$$\max_{w_1, w_2, \dots, w_{k-1} \in \mathbb{R}^n} \min_{\substack{z \neq 0, z \in \mathbb{R}^n \\ z \perp w_1, w_2, \dots, w_{k-1}}} \frac{z^\top F z}{z^\top z} = \lambda_k(F)$$

\diamond

As a particular case of Courant-Fischer theorem, taking $k = 2$ and $w_1 = \mathbb{1}_N$ we can find an upper bound to the second eigenvalue of the Laplacian: for a vector $z \in \mathbb{R}^m$ such that $z \perp \mathbb{1}$

$$\lambda_2(L) \leq \frac{z^\top L z}{z^\top z}$$

Therefore, defining $\lambda_2 \triangleq \lambda_2(L)$, we obtain a vector inequality, that will be used further on:

$$z^\top z \lambda_2 \leq z^\top L z \tag{2.1}$$

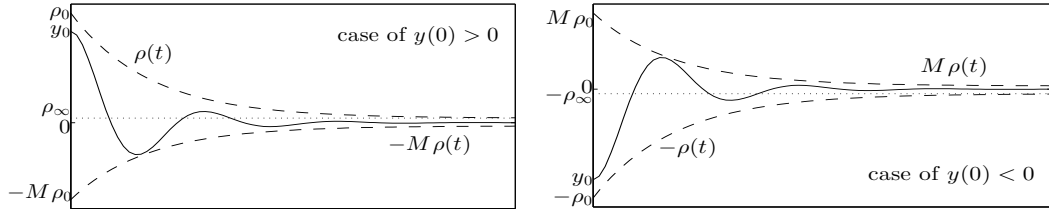


Figure 2.2: Performance bounds (dashed lines).

2.2 Prescribed performance control

In this section we will introduce the theoretical background for prescribed performance control ([16], [17]). The objective is to prescribe the evolution of a certain quantity of the system, e.g. the output, within certain bounds, guaranteeing its convergence to a predefined arbitrarily small set with a chosen convergence rate and a limited overshoot. The bounds are defined using functions $\rho(t) : \mathbb{R}_+ \rightarrow \mathbb{R}_+ \setminus \{0\}$ which are

1. positive, smooth and decreasing functions
2. s.t. $\lim_{t \rightarrow \infty} \rho(t) = \rho_\infty > 0$

and called *performance functions*. Let $y = [y_1, y_2, \dots, y_n]^\top$ denote the quantity (be it a state, an output or a function of them) whose time evolution we want to bound. The control objective is equivalent to

$$-M_i \rho_i(t) < y_i(t) < \rho_i(t) \quad \text{if } y_i(0) > 0 \quad (2.2a)$$

$$-\rho_i(t) < y_i(t) < M_i \rho_i(t) \quad \text{if } y_i(0) < 0 \quad (2.2b)$$

for all $t \geq 0$, where M_i is the maximum allowed overshoot for the i -th component.

Remark 2.1. ρ_∞ represents the maximum allowable error from the desired value of $y(t)$ at the steady state, while the rate of descent of the performance function is a lower bound on the speed of convergence. \triangleleft

Example 2. An exponentially decreasing function $\rho(t)$ satisfying the previously stated properties is

$$\rho(t) = (\rho_0 - \rho_\infty) e^{-\tau t} + \rho_\infty \quad (2.3)$$

with ρ_0 , ρ_∞ and τ appropriate constants. A graphical representation of the bounds (2.2) is shown in Figure 2.2. \triangle

By normalizing $y_i(t)$ with respect to the performance function we get the *modulated* (or *modified*) variable

$$\hat{y}_i(t) \triangleq \frac{y_i(t)}{\rho_i(t)} \quad (2.4)$$

and we can define the corresponding *prescribed performance regions*

$$D_{\hat{y}_i} \triangleq \{\hat{y}_i(t) : \hat{y}_i(t) \in (-M_i, 1)\} \quad \text{if} \quad \hat{y}_i(0) \geq 0 \quad (2.5a)$$

$$D_{\hat{y}_i} \triangleq \{\hat{y}_i(t) : \hat{y}_i(t) \in (-1, M_i)\} \quad \text{if} \quad \hat{y}_i(0) < 0 \quad (2.5b)$$

that are equivalent to (2.2).

We now introduce a function T_i of the modulated variable, called *transformation function*, with the following properties:

1. $T_i : D_{\hat{y}_i} \rightarrow \mathbb{R}$ is smooth and strictly increasing
2.
$$\left. \begin{array}{l} \lim_{\hat{y}_i \rightarrow -M_i} T_i(\hat{y}_i) = -\infty \\ \lim_{\hat{y}_i \rightarrow 1} T_i(\hat{y}_i) = +\infty \end{array} \right\} \quad \text{if} \quad y_i(0) > 0$$

$$\left. \begin{array}{l} \lim_{\hat{y}_i \rightarrow -1} T_i(\hat{y}_i) = -\infty \\ \lim_{\hat{y}_i \rightarrow M_i} T_i(\hat{y}_i) = +\infty \end{array} \right\} \quad \text{if} \quad y_i(0) < 0$$

for $i = 1, 2, \dots, n$. Then we denote with

$$\varepsilon_i(\hat{y}_i) = T_i(\hat{y}_i) \quad (2.6)$$

the *transformed* variable, where we dropped the time argument t from $\hat{y}_i(t)$ for notation convenience. We additionally define the stack vector of all transformed variables

$$\varepsilon(\hat{y}) = [\varepsilon_1(\hat{y}_1), \varepsilon_2(\hat{y}_2), \dots, \varepsilon_n(\hat{y}_n)]^\top \quad (2.7)$$

The domain of the vector function $\varepsilon(\hat{y})$ is the Cartesian product

$$D_{\hat{y}} = D_{\hat{y}_1} \times D_{\hat{y}_2} \times \dots \times D_{\hat{y}_m}$$

Differentiating (2.6) with respect to time, we obtain

$$\dot{\varepsilon}_i(\hat{y}_i) = \mathcal{J}_{T_i}(\hat{y}_i, t) [\dot{y}_i + \alpha_i(t)\hat{y}_i] \quad (2.8)$$

where

$$\mathcal{J}_{T_i}(\hat{y}_i, t) \triangleq \frac{\partial T_i(\hat{y}_i)}{\partial \hat{y}_i} \frac{1}{\rho_i(t)} > 0 \quad (2.9)$$

$$\alpha_i(t) \triangleq -\frac{\dot{\rho}_i(t)}{\rho_i(t)} \quad (2.10)$$

for $i = 1, \dots, n$ are, respectively, the *the normalized Jacobian* of the transformation T_i and the normalized derivative of the performance function. The functions $\alpha_i(t) \geq 0$,

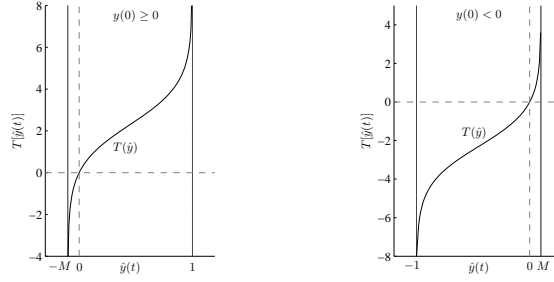


Figure 2.3: Error transformation with natural logarithm.

with domain $D_{\hat{y}_i}$ are such that $\lim_{t \rightarrow \infty} \alpha_i(t) = 0$ for $i = 1, \dots, n$.

We also denote with

$$\mathcal{J}_T(\hat{y}, t) \triangleq \text{diag} \{ \mathcal{J}_{T_1}(\hat{y}_1, t), \mathcal{J}_{T_2}(\hat{y}_2, t), \dots, \mathcal{J}_{T_n}(\hat{y}_n, t) \} \quad (2.11)$$

the diagonal matrix of all the normalized Jacobians, with

$$P(t) \triangleq \text{diag} \{ \rho_1(t), \rho_2(t), \dots, \rho_n(t) \} \quad (2.12)$$

$$\dot{P}(t) \triangleq \text{diag} \{ \dot{\rho}_1(t), \dot{\rho}_2(t), \dots, \dot{\rho}_n(t) \} \quad (2.13)$$

$$P^{-1}(t) \triangleq \text{diag} \left\{ \frac{1}{\rho_1(t)}, \frac{1}{\rho_2(t)}, \dots, \frac{1}{\rho_n(t)} \right\} \quad (2.14)$$

the diagonal matrices of all the performance functions, their derivatives and their inverse functions, respectively. Finally we denote with

$$A(t) \triangleq \text{diag} \left\{ -\frac{\dot{\rho}_1(t)}{\rho_1(t)}, -\frac{\dot{\rho}_2(t)}{\rho_2(t)}, \dots, -\frac{\dot{\rho}_n(t)}{\rho_n(t)} \right\} = \dot{P}(t)P^{-1}(t) \quad (2.15)$$

the diagonal matrix of all the $\alpha_i(t)$ functions.

If the transformation function is such that $T_i(0) = 0$, an inequality, useful for stability analysis, is implied (cfr. [18]):

$$y_i^\top \mathcal{J}_{T_i}(\hat{y}_i, t) \varepsilon_i(\hat{y}_i) \geq \mu_{1,i} \varepsilon_i^2(\hat{y}_i) \quad (2.16)$$

for some positive constant $\mu_{1,i}$ for $i = 1, 2, \dots, N$.

Example 3. As suggested in [18] and [20], a possible transformation function can be

$$T(\hat{y}) = \begin{cases} \ln \left(\frac{M+\hat{y}}{M(1-\hat{y})} \right) & \text{if } y(0) > 0 \\ \ln \left(\frac{M(1+\hat{y})}{M-\hat{y}} \right) & \text{if } y(0) < 0 \end{cases} \quad (2.17)$$

Either the first or the second expression can be used if $y(0) = 0$ (Figure 2.3).

Note that with such a transformation we cannot set $M = 0$, because otherwise the transformation function would be infinite for any value of \hat{y}_i within the domain.

If we do not want to allow overshoot, we can use a transformation function of the form (cfr. [18], [20])

$$T(\hat{y}) = \begin{cases} \ln\left(\frac{M+\hat{y}}{1-\hat{y}}\right) & \text{if } y(0) > 0 \\ \ln\left(\frac{M-\hat{y}}{1+\hat{y}}\right) & \text{if } y(0) < 0 \end{cases} \quad (2.18)$$

△

2.3 Problem formulation

In this work we will consider a group of N agents each one described with a double-integrator model

$$\begin{aligned} \dot{x}_i &= v_i \\ \dot{v}_i &= u_i \end{aligned} \quad (2.19)$$

where $x_i \in \mathbb{R}$ is the position and $v_i \in \mathbb{R}$ is the velocity of the i -th agent, for $i = 1, \dots, N$. $u_i \in \mathbb{R}$ is the control input which, in such a model, corresponds to the acceleration of the agent. System (2.19) can be alternatively written as

$$\ddot{x}_i = u_i \quad (2.20)$$

For $k = 1, 2, \dots, m$ we define the *position error* (or relative position) between two communicating agents as

$$\bar{x}_k \triangleq x_{ij} = x_i - x_j \quad \text{with } j \in \mathcal{N}_i$$

In order to put the model of the multi-agent system in a vector form, we need to define:

- ▷ $x = [x_1, x_2, \dots, x_N]^\top$ as the stack vector of absolute positions of the agents.
- ▷ $v = \dot{x} = [v_1, v_2, \dots, v_N]^\top$ as the stack vector of absolute velocities of the agents.
- ▷ $\bar{x} = [\bar{x}_1, \bar{x}_2, \dots, \bar{x}_m]^\top$ as the stack vector of relative positions between pair of agents that form an edge in \mathcal{G} . Hence the following relation holds

$$\bar{x} = B^\top x \quad (2.21)$$

We also denote with

$$\bar{v}_k \triangleq v_{ij} = v_i - v_j \quad \text{with } j \in \mathcal{N}_i$$

the *velocity error* (or relative velocity) between two neighbouring agents. Therefore

▷ $\bar{v} = [\bar{v}_1, \bar{v}_2, \dots, \bar{v}_m]^\top$ is the stack vector of relative velocities between pair of agents that form an edge in \mathcal{G} and the following identity holds

$$\bar{v} = B^\top v \tag{2.22}$$

In a multi-agent system, the agents are supposed to communicate between each other with an arbitrary connection topology, which affects the behaviour and the stability properties of the system. Concerning this aspect, the main assumption we make is that the topology is time-invariant and all the communicating agents mutually exchange their current positions and velocities. We can summarize this in the following

Assumption 1. *The communication topology of the multi-agent system is described by a static graph with bidirectional links.*

The objective of this thesis is to provide a solution for these two problems:

Problem 1. Design a distributed controller for system (2.19) able to guarantee

- 1) Consensus of the position of the agents, i.e. ensuring that the trajectories of the agents will meet at a certain point.
- 2) Prescribed transient evolution of the position errors between two communicating agents.

In the last part of the thesis another control objective will be added, resulting in

Problem 2. Design a distributed controller for system (2.19) able to guarantee

- 1) Consensus of the position of the agents.
- 2) Prescribed transient evolution of the position errors between two communicating agents.
- 3) Prescribed transient evolution of the velocity errors between two communicating agents.

Chapter 3

Prescribed transient behaviour for the position errors: approach with absolute velocities

3.1 Proposed controller

For each agent, the proposed controller is the composition of a term based on prescribed performance of the position errors between the neighbouring agents and a second term which is proportional to the absolute velocity of the agent:

$$u_i = - \sum_{j \in \mathcal{N}_i} g_{ij} \mathcal{J}_{T_{ij}}(\hat{x}_{ij}, t) \varepsilon_{ij}(\hat{x}_{ij}) - \gamma v_i \quad i \in \mathcal{V} \quad (3.1)$$

with g_{ij} and γ being positive constants. The terms $\mathcal{J}_{T_{ij}}(\hat{x}_{ij}, t)$ and \hat{x}_{ij} have been defined in Section 2. The position errors x_{ij} are modulated by the performance functions $\rho_{ij}(t)$ and then transformed with $T_{ij}(\cdot) \triangleq \varepsilon_{ij}(\cdot)$. The corresponding allowed overshoot is denoted with M_{ij} .

Independence of the evolution of the *centroid*¹ of the prescribed performance term can be ensured by making the following assumptions:

Assumption 2. *The graph \mathcal{G} describing the communication topology of the multi-agent system is connected.*

Assumption 3. *For each pair of communicating agents the performance functions and the overshoot indices are the same, i.e. $\rho_{ij}(t) = \rho_{ji}(t)$ and $M_{ij} = M_{ji}$, and the transformation functions are such that $T_{ji}(\hat{x}_{ji}) = -T_{ij}(-\hat{x}_{ij})$.*

¹The *centroid* is defined as the average of the positions of the agents forming the system

This choice implies $\mathcal{J}_{T_{ij}}(\hat{x}_{ij}, t)\varepsilon_{ij}(\hat{x}_{ij}) = -\mathcal{J}_{T_{ji}}(\hat{x}_{ji}, t)\varepsilon_{ij}(\hat{x}_{ji})$ (cfr. [20]).

The system (2.19) with the control input (3.1) can be written in vector form as follows:

$$\begin{aligned}\dot{x} &= v \\ \dot{v} &= -B\mathcal{J}_T(\hat{x}, t)G\varepsilon(\hat{x}) - \gamma v\end{aligned}\tag{3.2}$$

or equivalently:

$$\ddot{x} = -B\mathcal{J}_T(\hat{x}, t)G\varepsilon(\hat{x}) - \gamma\dot{x}\tag{3.3}$$

where $G \in \mathbb{R}^{m \times m}$ is a positive definite diagonal gain matrix with entries g_{ij} . The matrix $\mathcal{J}_T(\hat{x}, t)$ and the vector $\varepsilon(\hat{x})$ are defined as (2.11) and (2.7), respectively.

In the following sections we will prove that the closed loop system (3.3) is stable, the consensus objective is achieved and the relative positions evolve within the performance bounds.

3.2 Time evolution of the centroid

In this section we investigate how the mean of the positions and the mean of the velocities of the agents of (3.2) vary during time by deriving an analytical expression that describes their evolution. We are also interested in their asymptotic value. The results we obtain are instrumental to the study of the equilibrium point of the controlled system. From now on $v_0 \triangleq v(0) \in \mathbb{R}^N$ is the vector of initial absolute velocities and $x_0 \triangleq x(0) \in \mathbb{R}^N$ is the vector of initial absolute positions of the agents.

Velocities

By multiplying both sides of the second equation in (3.2) by $\mathbb{1}_N^T$, we obtain

$$\mathbb{1}_N^T \dot{v} = -\mathbb{1}_N^T B \mathcal{J}_T(\hat{x}, t) G \varepsilon(\hat{x}) - \gamma \mathbb{1}_N^T \dot{x}$$

and therefore

$$\frac{d}{dt} \left(\sum_{i=1}^N v_i \right) = -\gamma \sum_{i=1}^N v_i\tag{3.4}$$

where the identity $\mathbb{1}_N^T B = 0$ was used. As explained, Assumption 3 implies that the evolution of the mean of both velocities and positions is independent of the prescribed performance term. In fact under this assumption, the incidence matrix B appears in the first control term. The linear differential equation (3.4) means that the sum of the

agents' velocities decreases exponentially during time, hence so does their mean

$$\frac{1}{N} \sum_{i=1}^N v_i(t) = \left(\frac{1}{N} \sum_{i=1}^N v_i(0) \right) e^{-\gamma t} \quad (3.5)$$

It is straightforward from (3.5) that the mean of the velocities will converge to zero asymptotically

$$\lim_{t \rightarrow \infty} \left(\frac{1}{N} \sum_{i=1}^N v_i(t) \right) = 0 \quad (3.6)$$

Positions

By multiplying both sides of the first equation in (3.2) by $\mathbb{1}_N^T$, we obtain

$$\begin{aligned} \mathbb{1}_N^T \dot{x} &= \mathbb{1}_N^T v \\ \frac{d}{dt} \left(\sum_{i=1}^N x_i \right) &= \sum_{i=1}^N v_i = e^{-\gamma t} \left(\frac{1}{N} \sum_{i=1}^N v_i(0) \right) \end{aligned} \quad (3.7)$$

Solving (3.7) by means of integration, we have

$$\begin{aligned} \int_0^t \sum_{i=1}^N \dot{x}_i(\tau) d\tau &= -\frac{1}{\gamma} \left(\sum_{i=1}^N v_i(0) \right) \int_0^t -\gamma e^{-\gamma\tau} d\tau \\ \sum_{i=1}^N x_i(t) - \sum_{i=1}^N x_i(0) &= -\frac{1}{\gamma} \left(\sum_{i=1}^N v_i(0) \right) (e^{-\gamma t} - 1) \end{aligned}$$

Therefore, the mean of the agents' positions evolves according to

$$c(t) = \frac{1}{N} \sum_{i=1}^N x_i(t) = \frac{1}{N} \sum_{i=1}^N x_i(0) - \frac{1}{\gamma} \left(\frac{1}{N} \sum_{i=1}^N v_i(0) \right) (e^{-\gamma t} - 1) \quad (3.8)$$

and asymptotically converges to

$$c_\infty = \lim_{t \rightarrow \infty} c(t) = \frac{1}{N} \sum_{i=1}^N x_i(0) + \frac{1}{\gamma} \left(\frac{1}{N} \sum_{i=1}^N v_i(0) \right) \quad (3.9)$$

that can be written in a vector form as:

$$c_\infty = \frac{1}{N} \mathbb{1}_N^T \left(x_0 + \frac{1}{\gamma} v_0 \right) \quad (3.10)$$

Based on this analysis, the centroid is time-variant and in particular it evolves exponentially from its initial value $c_0 = \frac{1}{N} \mathbb{1}_N^T x_0$ to its final value c_∞ . Note that if the sum of initial velocities is zero, then the time-dependent term of (3.8) vanishes and the the mean of the agents' positions becomes time-invariant, i.e. $c(t) = c_0 = c_\infty$ for $t \geq 0$.

3.3 Stability analysis

The controller (3.1) introduces a dependence on time and alters the linearity of (2.19), transforming the original system in a nonlinear and time-variant one. We will use Lyapunov-like tools in order to prove that the controlled system is stable and at the same time consensus and prescribed performance are guaranteed.

Before stating the main result we need to introduce a change in the notation: instead of using x_{ij} and $\rho_{ij}(t)$, we denote the performance function associated to the position error \bar{x}_k between two neighbouring agents with $\rho_k(t)$.

Theorem 3.1. *Consider the prescribed performance agreement protocol (3.1) applied to the double integrator dynamics (2.19) under Assumptions 1,2 and 3. Consider also performance functions $\rho_k(t)$ with bounded derivative and transformation functions s.t. $T_k(0) = 0$ for all k .*

If 1) the condition

$$\gamma > \max_{t \geq 0} \alpha_k(t) \quad (3.11)$$

holds $\forall k$ and 2) the initial conditions $\bar{x}_k(0)$ are inside the performance bounds (2.2) for $k = 1, \dots, m$, then

i) the relative errors $\bar{x}_k(t)$ will evolve within the prescribed performance bounds for $k = 1, \dots, m$ and $\forall t \geq 0$,

ii) the relative errors $x_k(t)$ will converge to zero for $k = 1, \dots, m$,

iii) the absolute velocities $v_i(t)$ will converge to zero for $i = 1, \dots, N$. \diamond

Proof. Let $\xi = [x^T v^T]^T$ be the state vector of (3.2). Consider an arbitrarily chosen positive constant θ and the following potential function

$$V(\xi, \hat{x}) = \frac{1}{2} \xi^T Q \xi + \frac{1}{2} \varepsilon^T(\hat{x}) G \varepsilon(\hat{x}) \quad (3.12)$$

where $Q = \begin{bmatrix} \theta\gamma I_N & \theta I_N \\ \theta I_N & I_N \end{bmatrix}$. V is positive definite if

$$\begin{cases} \theta\gamma > 0 \\ \theta(\gamma - \theta) > 0 \end{cases} \quad \text{and therefore if} \quad \begin{cases} \theta > 0 \\ \gamma > \theta \end{cases} \quad (3.13)$$

Differentiating (3.12) along the trajectories of (3.3) and considering (2.8) we obtain

$$\dot{V}(\xi, \hat{x}) = -[\theta I_m - A(t)] \bar{x}^T \mathcal{J}_T(\hat{x}, t) G \varepsilon(\hat{x}) - (\gamma - \theta) v^T v \quad (3.14)$$

which is negative semi-definite when (3.13) holds and

$$[\theta I_m - A(t)] > 0 \quad (3.15)$$

where $A(t)$ is the $m \times m$ diagonal matrix with entries $\alpha_k(t) = -\frac{\dot{\rho}_k(t)}{\rho_k(t)}$. Condition (3.13) and (3.15) together give (3.11) and since $\dot{\rho}_k(t)$ is bounded $\forall k$, this ensures that $\max_{t \geq 0} \alpha_k(t) < \infty$. Hence if (3.11) is satisfied, \dot{V} is negative semi-definite and this implies that $V(\xi, \hat{x}) \leq V(\xi(0), \hat{x}(0))$ which in turn implies that $\xi, \varepsilon(\hat{x}) \in \mathcal{L}_\infty$, given that $V(\xi(0), \hat{x}(0))$ is bounded. Therefore, if $\hat{x}(0)$ is chosen within the regions (2.5) then $V(\xi(0), \hat{x}(0))$ is finite, $\varepsilon(\hat{x}) \in \mathcal{L}_\infty$ and consequently $\bar{x}(t)$ evolves within the prescribed performance bounds $\forall t$. Thus, we have proved *i*).

Computing the second derivative of $V(\xi, \hat{x})$, we can conclude that it is bounded based on the fact that $\varepsilon(\hat{x})$ and $\dot{\varepsilon}(\hat{x})$ are bounded. Boundedness of $\ddot{V}(\xi, \hat{x})$ implies that $\dot{V}(\xi, \hat{x})$ is uniformly continuous and therefore, by applying Barbalat's Lemma, $\dot{V}(\xi, \hat{x}) \rightarrow 0$ as $t \rightarrow \infty$. This means that the trajectories of (3.3) will converge to the set in which \dot{V} is equal to zero, that is $E = \{(v, \hat{x}) \mid v = 0, \hat{x} = 0\}$ (note that the derivative does not depend on the absolute positions). If the transformation functions T_k are chosen such that $T_k(0) = 0 \forall k$, then $\dot{V}(\xi, \hat{x}) \rightarrow 0$ implies $\bar{x} \rightarrow 0$ and $v \rightarrow 0$ as $t \rightarrow \infty$. This proves *ii*) and *iii*). \square

Theorem 3.1 states that under certain assumptions the multi-agents system will asymptotically reach consensus, but still does not say anything about the actual value of the absolute positions at the equilibrium. In that sense the Corollary below fills this gap:

Corollary 3.2. *The prescribed performance agreement protocol (3.1) applied to the multi-agent system (2.19), under all the assumptions of Theorem 3.1 ensures the convergence of the agents' absolute positions to the centroid. \diamond*

Proof. Equation (3.9) yields

$$\begin{aligned} \lim_{t \rightarrow \infty} [\mathbb{1}_N^T x(t)] &= \mathbb{1}_N^T \left(x_0 + \frac{1}{\gamma} v_0 \right) \\ \mathbb{1}_N^T x_\infty &= \beta \end{aligned} \quad (3.16)$$

On the other hand from Theorem 3.1 we know that the agents will asymptotically reach the same absolute position

$$x_\infty = \mathbb{1}_N \vartheta \quad (3.17)$$

and need to find which is the value of the constant ϑ . By combining (3.16) and (3.17) we obtain the following linear system:

$$\begin{bmatrix} I_N & -\mathbb{1}_N \\ \mathbb{1}_N^T & 0 \end{bmatrix} \begin{bmatrix} x_\infty \\ \vartheta \end{bmatrix} = \begin{bmatrix} \mathbf{0}_N \\ \beta \end{bmatrix} \quad (3.18)$$

which is a Cramer's system and has only one solution, given by

$$\vartheta = \frac{1}{N} \det \left(\begin{bmatrix} I_N & \mathbf{0}_N \\ \mathbb{1}_N^T & \beta \end{bmatrix} \right) = \frac{1}{N} \beta = c_\infty \quad (3.19)$$

where we used the identity $\det \begin{pmatrix} E & F \\ G & H \end{pmatrix} = \det(E) \det(H - GE^{-1}F)$ that holds for every E invertible. \square

Details about how the function (3.12) was obtained are shown in Appendix A. For the expression of \ddot{V} see Appendix B.

3.4 Simulations

In this sections simulation results are presented in order to validate the theoretical findings of the previous sections. We consider $N = 6$ agents moving on a planar surface. Let $p_i = [x_i \ y_i]^T$, $i \in \{1, 2, \dots, N\}$, be the position of each agent and let d denote the sum of the distances between the agents and the centroid

$$d \triangleq \sum_{i=1}^6 \|p_i - p_c\|$$

with $p_c \triangleq \frac{1}{6} \sum_{i=1}^6 p_i$. The positions errors are modulated by an exponentially decreasing performance function

$$\rho_k(t) = \rho(t) = (\rho_0 - \rho_\infty) \exp^{-\tau t} + \rho_\infty \quad \text{for } k = 1, 2, \dots, m$$

which is the same for all the pairs of connected agents, and then transformed by the logarithmic function

$$T(\hat{x}) = \begin{cases} \ln \left(\frac{M + \hat{x}}{M(1 - \hat{x})} \right) & \text{if } \hat{x}(0) > 0 \\ \ln \left(\frac{M(1 + \hat{x})}{M - \hat{x}} \right) & \text{if } \hat{x}(0) < 0 \end{cases} \quad (3.20)$$

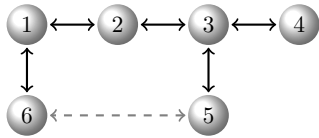


Figure 3.1: Communication graph of the multi-agent system used in the simulations: spanning tree \mathcal{G}_1 in solid lines and connected graph with one cycle \mathcal{G}_2 in solid and dashed lines.

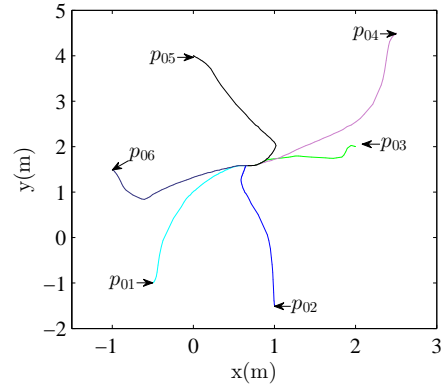


Figure 3.2: Agents trajectories on the $x - y$ plane for PPC1 in case of \mathcal{G}_1 , with $\gamma = 250$ and $G = 36.5I_m$.

already presented in Section 2.2. With this performance function the condition (3.11), sufficient for the convergence of the trajectories of (3.3), becomes

$$\gamma > \tau \left(\frac{\rho_0 - \rho_\infty}{\rho_0} \right) \quad (3.21)$$

By choosing $\rho_0 = 8$, $\rho_\infty = 10^{-2}$, $M = 0.1$ and $\tau = 2$ the condition on the damping becomes $\gamma > 1.9975$. Furthermore we set the maximum allowed overshoot to $M = 0.1$. We also consider three different topologies for the connection between the agents: a spanning tree (\mathcal{G}_1) and connected graph with a cycle (\mathcal{G}_2), shown in Figure 3.1, and also a complete graph (\mathcal{G}_3). Note that in all the proposed cases we have a connected graph, satisfying Assumption 2. The initial positions of the agents are: $p_{01} = [-0.5 \ -1]^T$, $p_{02} = [1 \ -1.5]^T$, $p_{03} = [2 \ 2]^T$, $p_{04} = [2.5 \ 4.5]^T$, $p_{05} = [0 \ 4]^T$, $p_{06} = [-1 \ 1.5]^T$. Given this set of initial conditions we have that $\bar{x}_k(0) < \rho_0$ and $\bar{y}_k(0) < \rho_0 \ \forall k$ and for each configuration of the communication graph. Furthermore the agents' initial velocities are equal to 0. The presented controller (PPC1) has been tuned with the following values for the parameters: $\gamma = 250$, $G = 36.5I_m$. With this settings, all the hypothesis of Theorem 3.1 are satisfied, therefore agreement and prescribed transient evolution are guaranteed and Corollary 3.2 ensures convergence to the centroid. The same Corollary gives the final consensus value, which is equal to the mean of initial conditions $c_\infty = \frac{1}{N} \sum_{i=1}^6 p_{i0} = [0.6667 \ 1.5833]^T$.

In Figure 3.2 the trajectories of the agents on the plane shown while in Figure 3.3 we can see that the relative positions evolve within the performance bounds. The large value of γ , that acts as a damping, avoids oscillations on the absolute velocities, and consequently on the relative velocities, but implies a slower response as the agents start to move (Figure 3.4). Repeated simulations with this settings (same $\rho(t)$, $T(\hat{\mathbf{x}})$ and M) have revealed that for values of γ lower than 80 the velocity response oscillates, especially when the system is approaching the steady state value (Figure 3.5). Note that when γ

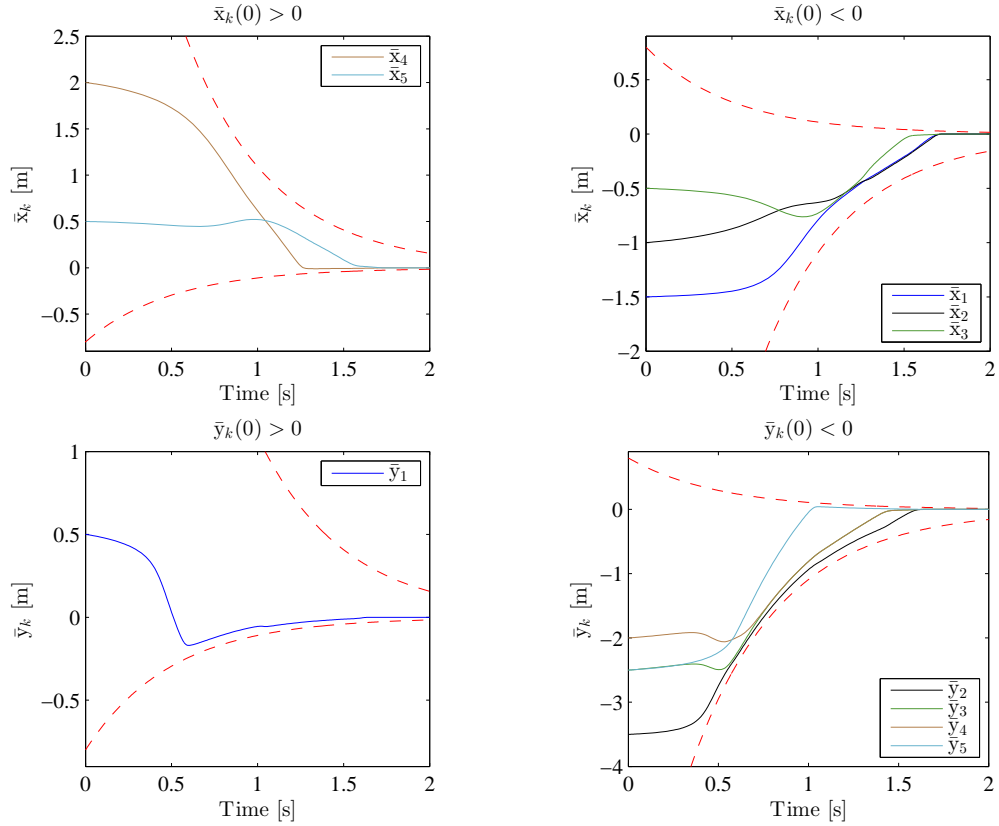


Figure 3.3: Relative positions (solid lines) and performance bounds (dashed lines) in case of \mathcal{G}_1 , with $\gamma = 250$ and $G = 36.5I_m$.

changes the gain matrix $G = \text{diag}\{g_k\}$ ² has to be re-tuned in order to have adequate values for the control inputs. In fact, the parameters g_k are scaling factors acting on the transformation functions T_k : their values can be adequately increased in order to reduce the value of $\varepsilon(\hat{x})$ and therefore avoid high control inputs. On the other hand if the transformed errors are smaller, this means that the distance between $\bar{x}(t)$ ($\bar{y}(t)$) and $\rho(t)$ is bigger, implying not only small inputs but also a faster convergence to 0 of the errors (Figure 3.6). Given the choice of the performance functions $\rho_k(t)$ each agent can know a priori the minimum rate of convergence of the system by setting the value of τ . However the choice of ρ_0 can further affect the time needed to reach consensus: in fact if $\rho_0 \gg \bar{x}_0, \bar{y}_0$, the agents will not start moving (or will slowly move) at the beginning because of the small contribution of $B\mathcal{J}_T(\hat{x}, t)G\varepsilon(\hat{x})$ and $B\mathcal{J}_T(\hat{y}, t)G\varepsilon(\hat{y})$ due to the fact that $\bar{x}(t)$ and $\bar{y}(t)$ evolve far from the performance bounds.

Regarding how the communication graph affects the properties of the proposed protocol, we can notice that increasing the number of connections between the agents the time required to reach consensus is reduced: this is particularly evident in the case of \mathcal{G}_3 (Figure 3.8).

² $g_k \triangleq g_{ij}$ for $k = 1, 2, \dots, m$, where k is the edge connecting agent i and j

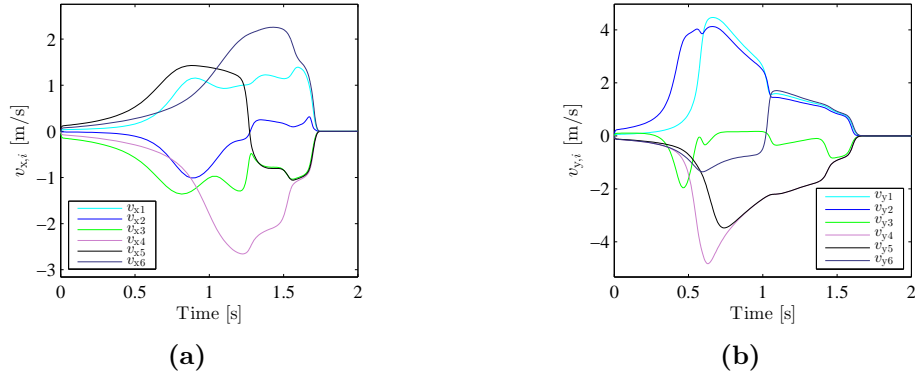


Figure 3.4: Absolute velocities along (a) x coordinate and (b) y coordinate in case of \mathcal{G}_1 , with $\gamma = 250$ and $G = 36.5I_m$.

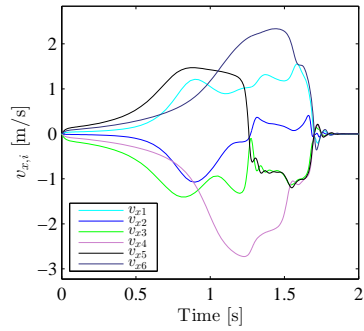


Figure 3.5: Absolute velocities along the x coordinate with $\gamma = 50$ and $G = 7.8I_m$, in case of \mathcal{G}_1 .

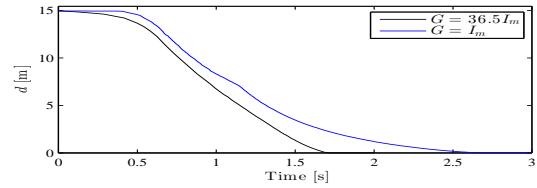


Figure 3.6: Response of the total distance from the centroid for PPC1 in the case of \mathcal{G}_1 : confront between $G = I_m$ and $G = 36.5I_m$.

We also compared the nonlinear protocol with the linear one $\dot{\xi} = \Gamma\xi$, where $\Gamma = \begin{bmatrix} \mathbf{0}_N & I_N \\ -L & -\gamma_L I_N \end{bmatrix}$. The value of the parameter γ_L has been chosen in order to guarantee the maximum rate of convergence possible with the considered configuration while avoiding oscillations³. Observing Figure 3.7, we can understand the advantages of the nonlinear protocol with respect to the linear one: in fact, by decoupling the speed of convergence from the graph topology, we can reach a much faster convergence by appropriately choosing the prescribed performance function. For \mathcal{G}_1 the value of the second smallest eigenvalue of Γ is $\lambda_{2+}(\Gamma) = -0.0787$ and this implies the slow convergence of the linear algorithm (order of $e^{\lambda_{2+}t}$): on the other hand, by using the nonlinear protocol and choosing an exponentially decreasing performance function with $\tau = 2$ we are able to guarantee a rate of convergence of the order of e^{-2t} , which is considerably faster.

³The eigenvalues of Γ directly depend on the eigenvalues of L and on the value of γ_L according to $\lambda_{i\pm}(\Gamma) = \frac{1}{2} \left(-\gamma_L \pm \sqrt{\gamma_L^2 - 4\lambda_i(L)} \right)$. Therefore, to guarantee that all the eigenvalue of Γ are real (to avoid oscillation) we have to choose $\gamma_L > 2\sqrt{\lambda_{\max}(L)}$. Note also that the value of $\lambda_{2+}(\Gamma)$ decreases as γ_L increases.

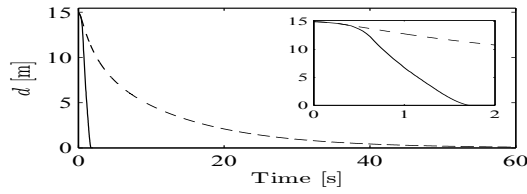


Figure 3.7: Comparison between PPC1 (solid line), with $\gamma = 250$ and $G = 36.5I_m$, and the linear protocol (dashed line). Case of \mathcal{G}_1 .

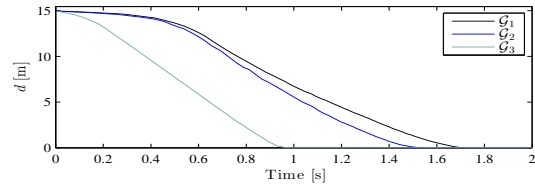


Figure 3.8: Comparison of PPC1 performance depending on the topology of connections between agents. Distance from the centroid. $\gamma = 250$ and $G = 36.5I_m$.

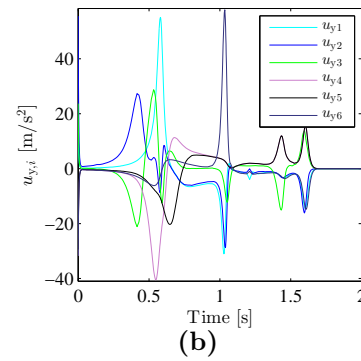
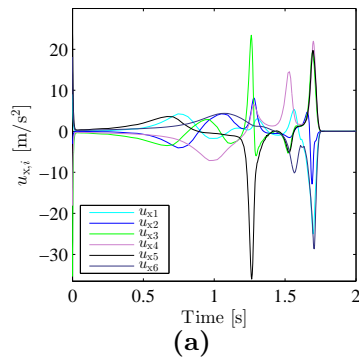


Figure 3.9: Control inputs along (a) x coordinate and (b) y coordinate in case of \mathcal{G}_1 , with $\gamma = 250$ and $G = 36.5I_m$.

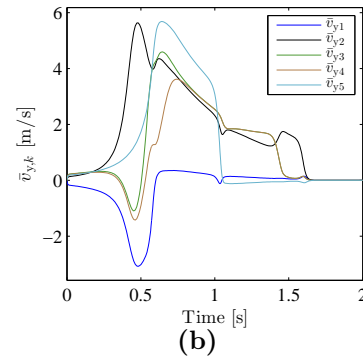
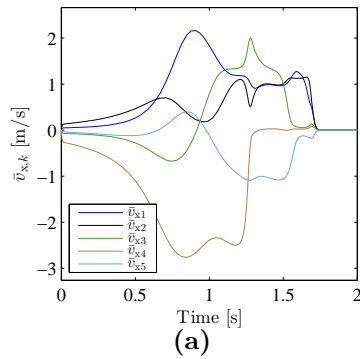


Figure 3.10: Relative velocities along (a) x coordinate and (b) y coordinate in case of \mathcal{G}_1 , with $\gamma = 250$ and $G = 36.5I_m$.

Chapter 4

Prescribed transient behaviour for the position errors: approach with relative velocities

4.1 Proposed controller

In this chapter we propose a control law which is similar to (3.1), consisting of the same term based on prescribed performance for the relative positions but using the relative velocities between neighbouring agents instead of the absolute velocities:

$$u_i = - \sum_{j \in \mathcal{N}_i} [g_{ij} \mathcal{J}_{T_{ij}}(\hat{x}_{ij}, t) \varepsilon_{ij}(\hat{x}_{ij}) + \gamma v_{ij}] \quad i \in \mathcal{V} \quad (4.1)$$

where all the terms are defined as before.

Considering Assumption 3 of the previous chapter, system (2.19) with the control (4.1) can be written in a vector form as follows:

$$\begin{aligned} \dot{x} &= v \\ \dot{v} &= -B \mathcal{J}_T(\hat{x}, t) G \varepsilon(\hat{x}) - \gamma B \bar{v} \end{aligned} \quad (4.2)$$

or equivalently:

$$\ddot{x} = -B \mathcal{J}_T(\hat{x}, t) G \varepsilon(\hat{x}) - \gamma B \dot{v} \quad (4.3)$$

$$\ddot{\tilde{x}} = -B^\top B \mathcal{J}_T(\hat{x}, t) G \varepsilon(\hat{x}) - \gamma B^\top B \dot{\tilde{x}} \quad (4.4)$$

4.2 Time evolution of the centroid

Same as in the previous case, we start the analysis of the controlled system (4.2) by investigating the time evolution of both the mean of the positions and the mean of the velocities of the agents. The results are instrumental for the stability analysis.

Velocities

By multiplying both sides of the second equation in (4.2) by $\mathbb{1}_N^\top$, we obtain

$$\mathbb{1}_N^\top \dot{v} = -\mathbb{1}_N^\top B \mathcal{J}_T(\hat{x}, t) G \varepsilon(\hat{x}) - \gamma \mathbb{1}_N^\top B v$$

and therefore

$$\frac{d}{dt} \left(\sum_{i=1}^N v_i \right) = 0 \quad (4.5)$$

where the identity $\mathbb{1}_N^\top B = 0$ has been used. The linear differential equation (4.5) implies that the sum of the agents' velocity is constant during time and equal to the sum of initial velocities, hence their mean evolves according to

$$\frac{1}{N} \sum_{i=1}^N v_i(t) = \frac{1}{N} \sum_{i=1}^N v_i(0) \quad (4.6)$$

which in vector form gives

$$\frac{1}{N} \mathbb{1}_N^\top v(t) = \frac{1}{N} \mathbb{1}_N^\top v_0 \quad (4.7)$$

Positions

By multiplying both sides of the first equation in (4.2) by $\mathbb{1}_N^\top$, we can obtain

$$\begin{aligned} \mathbb{1}_N^\top \dot{x} &= \mathbb{1}_N^\top v \\ \frac{d}{dt} \left(\sum_{i=1}^N x_i \right) &= \sum_{i=1}^N v_i = \frac{1}{N} \sum_{i=1}^N v_i(0) \end{aligned} \quad (4.8)$$

Solving (4.8) by means of integration, we get

$$\begin{aligned} \int_0^t \sum_{i=1}^N \dot{x}_i(\tau) d\tau &= \int_0^t \sum_{i=1}^N v_i(0) d\tau \\ \sum_{i=1}^N x_i(t) - \sum_{i=1}^N x_i(0) &= \left(\sum_{i=1}^N v_i(0) \right) t \end{aligned}$$

Therefore, the mean of agents' positions (i.e. the *centroid*) evolves according to

$$c_\infty(t) = \frac{1}{N} \sum_{i=1}^N x_i(t) = \frac{1}{N} \sum_{i=1}^N x_i(0) - \left(\frac{1}{N} \sum_{i=1}^N v_i(0) \right) t \quad (4.9)$$

that can be written in a vector form as follows:

$$\frac{1}{N} \mathbb{1}_N^\top x(t) = \frac{1}{N} \mathbb{1}_N^\top x_0 - \left(\frac{1}{N} \mathbb{1}_N^\top v_0 \right) t \quad (4.10)$$

Unlike in the previous solution, if the sum of initial velocities is not zero the centroid does not converge to a constant value. This is a direct consequence of the fact that the controller includes the relative rather than the absolute velocities.

Before proceeding with studying the stability of the system, we need to state the following assumption:

Assumption 4. *The sum of all initial absolute velocities of the agents is equal to 0, or equivalently v_0 is such that $\mathbb{1}_N^\top v_0 = 0$.*

Note that the latter condition is not too restrictive, since in most of the applications the agents start with zero velocity. Given that Assumption 4 holds we can prove the following Lemma:

Lemma 4.1. *Consider the multi-agent system (2.19) with the prescribed performance agreement control protocol (4.1). Under Assumptions 1, 2, 3 and 4 the value of the centroid remains constant and equal to $c_x = \frac{1}{N} \sum_{i=1}^N x_i(0)$ during the motion. \diamond*

Proof. The proof is straightforward from equation (4.10), which under Assumption 4 becomes

$$\frac{1}{N} \mathbb{1}_N^\top x(t) = \frac{1}{N} \mathbb{1}_N^\top x_0 = c_x \quad (4.11)$$

□

4.3 Stability analysis

By using a simple change of coordinates, we construct an equivalent model of (4.2) where the state given by the difference between the state vector ξ and the equilibrium. Instead of studying the stability of the system (4.2), we prove the convergence to zero of this system.

Let us denote with $\xi^* = \begin{bmatrix} x^* \\ v^* \end{bmatrix}$ the equilibrium point of the controlled system, that satisfies the equation $\dot{\xi}^* = 0$. From the first and second equation of (4.2) we get:

$$v^* = 0 \quad (4.12a)$$

$$\bar{v} = B^\top v^* = 0 \quad \text{and} \quad \bar{x}^* = B^\top x^* = 0 \quad (4.12b)$$

From (4.12b), x^* has to be parallel to the vector $\mathbb{1}_N$, i.e. $x^* = a\mathbb{1}_N$, $a \in \mathbb{R}$. Furthermore, from (4.11) we know that $\mathbb{1}_N^\top x = \mathbb{1}_N^\top x_0$, then

$$\mathbb{1}_N^\top x = a\mathbb{1}_N^\top \mathbb{1}_N \quad \Rightarrow \quad \mathbb{1}_N^\top x_0 = Na \quad \Rightarrow \quad a = \frac{1}{N} \mathbb{1}_N^\top x_0 = c_x$$

Therefore the equilibrium is given by

$$\begin{bmatrix} x^* \\ v^* \end{bmatrix} = \begin{bmatrix} c_x \mathbb{1}_N \\ \mathbf{0}_N \end{bmatrix} \quad (4.13)$$

We are now ready to define the *disagreement vector*

$$\mathbf{e} = \begin{bmatrix} \mathbf{e} \\ \dot{\mathbf{e}} \end{bmatrix} = \begin{bmatrix} x - x^* \\ v - v^* \end{bmatrix} = \begin{bmatrix} x - c_x \mathbb{1}_N \\ v \end{bmatrix} \quad (4.14)$$

which clearly satisfies the following identities

$$\begin{aligned} x &= \mathbf{e} + c_x \mathbb{1}_N \\ \bar{x} &= B^\top x = B^\top \mathbf{e} \triangleq \bar{\mathbf{e}} \\ \bar{v} &= B^\top v = B^\top \dot{\mathbf{e}} \triangleq \dot{\bar{\mathbf{e}}} \end{aligned}$$

and the *disagreement dynamics*

$$\begin{aligned} \dot{\mathbf{e}} &= v \\ \ddot{\mathbf{e}} &= -B\mathcal{J}_T(\hat{\mathbf{e}}, t)G\varepsilon(\hat{\mathbf{e}}) - \gamma B\dot{\mathbf{e}} \end{aligned} \quad (4.15)$$

where $\hat{\mathbf{e}}(t) \triangleq \left[\frac{\bar{\mathbf{e}}_1^\top(t)}{\rho_1(t)}, \frac{\bar{\mathbf{e}}_2^\top(t)}{\rho_2(t)}, \dots, \frac{\bar{\mathbf{e}}_m^\top(t)}{\rho_m(t)} \right]^\top = P^{-1}(t)\bar{\mathbf{e}}(t)$.

The previous definitions also suggest the following inequality

$$\|\bar{\mathbf{e}}\| = \|\bar{x}\| \leq \|B\| \|(x - c_x \mathbb{1}_N)\| = \|B\| \|\mathbf{e}\| \quad (4.16)$$

relating the norm of the disagreement vector in the edge space with the one in the vertex space. Another useful inequality can be derived as a consequence of Courant-Fischer

theorem, giving a lower bound on the eigenvalue $\lambda_2 \triangleq \lambda_2(L)$ (cfr. Section 2.1)

$$\lambda_2(L) = \min_{e: e \perp \mathbb{1}_N} \frac{e^\top L e}{e^\top e}$$

and consequently yielding

$$e^\top e \lambda_2 \leq \bar{e}^\top \bar{e} \quad (4.17)$$

which, since $e \perp \mathbb{1}_N \forall e \neq 0$, is always valid. Furthermore, exploiting again Courant-Fischer theorem, the inequality

$$\dot{e}^\top \dot{e} \lambda_2 \leq \dot{\bar{e}}^\top \dot{\bar{e}} \quad (4.18)$$

is valid $\forall \dot{e}$ if Assumption 4 holds.

A comprehensive result on stability and consensus achievement with prescribed performance guarantees can now be stated:

Theorem 4.2. *Consider the prescribed performance agreement protocol (4.1) applied to the double integrator dynamics (2.19) under Assumptions 1,2,3 and 4. Consider also performance functions $\rho_k(t)$ with bounded derivative and transformation functions s.t. $T_k(0) = 0$ for all k .*

If 1) the condition

$$\gamma > \frac{1}{\lambda_2(L)} \max_{t \geq 0} \alpha_k(t) \quad (4.19)$$

holds $\forall k$ and 2) the initial conditions $\bar{x}_k(0)$ are within the performance bounds (2.2) for $k = 1, \dots, m$, then

i) the relative errors $\bar{x}_k(t)$ will evolve within the prescribed performance bounds for $k = 1, \dots, m$,

ii) the trajectories will converge to the equilibrium (4.13). \diamond

Proof. To prove stability of the equilibrium we investigate the disagreement dynamics (4.15) considering the following Lyapunov function candidate

$$V(\mathbf{e}, \hat{\mathbf{e}}) = \frac{\theta\gamma}{2} \bar{\mathbf{e}}^\top \bar{\mathbf{e}} + \theta \mathbf{e}^\top \dot{\mathbf{e}} + \frac{1}{2} \dot{\mathbf{e}}^\top \dot{\mathbf{e}} + \frac{1}{2} \varepsilon^\top (\hat{\mathbf{e}}) G \varepsilon (\hat{\mathbf{e}}) \quad (4.20)$$

with θ arbitrarily chosen positive constant. $V(\mathbf{e}, \hat{\mathbf{e}})$ is such that $V(0, 0) = 0$ and in order to prove that it is also positive definite we will proceed by bounding it from above and below with two positive definite functions. By taking into account inequality (4.16) and

¹By definition $\mathbf{e} = x - c_x \mathbb{1}_N$ and then $\mathbb{1}_N^\top \mathbf{e} = \mathbb{1}_N^\top x - (\frac{1}{N} \mathbb{1}_N^\top x_0) \mathbb{1}_N^\top \mathbb{1}_N = \mathbb{1}_N^\top x - \mathbb{1}_N^\top x_0 = 0$ as a consequence of Lemma 4.1

$\|B\|^2 = \lambda_{\max}(L_E) \triangleq \lambda_M$: we can bound $V(\mathbf{e}, \hat{\mathbf{e}})$ from above with a function $W_2(\mathbf{e}, \hat{\mathbf{e}})$

$$\begin{aligned} V(\mathbf{e}, \hat{\mathbf{e}}) &\leq W_2(\mathbf{e}, \hat{\mathbf{e}}) = \frac{\theta\gamma}{2}\lambda_M \mathbf{e}^\top \mathbf{e} + \theta \mathbf{e}^\top \dot{\mathbf{e}} + \frac{1}{2}\dot{\mathbf{e}}^\top \dot{\mathbf{e}} + \frac{1}{2}\varepsilon^\top(\hat{\mathbf{e}})G\varepsilon(\hat{\mathbf{e}}) \\ &= \frac{1}{2} \begin{bmatrix} \mathbf{e} \\ \dot{\mathbf{e}} \end{bmatrix}^\top \begin{bmatrix} \theta\gamma\lambda_M I_N & \theta I_N \\ \theta I_N & I_N \end{bmatrix} \begin{bmatrix} \mathbf{e} \\ \dot{\mathbf{e}} \end{bmatrix} + \frac{1}{2}\varepsilon^\top(\hat{\mathbf{e}})G\varepsilon(\hat{\mathbf{e}}) \end{aligned} \quad (4.21)$$

such that $W_2(0, 0) = 0$, which is positive definite if

$$\begin{cases} \theta\gamma\lambda_M > 0 \\ \theta(\gamma\lambda_M - \theta) > 0 \end{cases} \quad \text{and therefore if} \quad \begin{cases} \theta > 0 \\ \gamma\lambda_M > \theta \end{cases} \quad (4.22)$$

Since $\lambda_2 > 0$, because the graph \mathcal{G} is connected (Theorem 2.8, [23]), we can use (4.17) to find a function $W_1(\mathbf{e}, \hat{\mathbf{e}})$ which represents a lower bound for $V(\mathbf{e}, \hat{\mathbf{e}})$

$$\begin{aligned} V(\mathbf{e}, \hat{\mathbf{e}}) &\geq W_1(\mathbf{e}, \hat{\mathbf{e}}) = \frac{\theta\gamma}{2}\lambda_2 \mathbf{e}^\top \mathbf{e} + \theta \mathbf{e}^\top \dot{\mathbf{e}} + \frac{1}{2}\dot{\mathbf{e}}^\top \dot{\mathbf{e}} + \frac{1}{2}\varepsilon^\top(\hat{\mathbf{e}})G\varepsilon(\hat{\mathbf{e}}) \\ &= \frac{1}{2} \begin{bmatrix} \mathbf{e} \\ \dot{\mathbf{e}} \end{bmatrix}^\top \begin{bmatrix} \theta\gamma\lambda_2 I_N & \theta I_N \\ \theta I_N & I_N \end{bmatrix} \begin{bmatrix} \mathbf{e} \\ \dot{\mathbf{e}} \end{bmatrix} + \frac{1}{2}\varepsilon^\top(\hat{\mathbf{e}})G\varepsilon(\hat{\mathbf{e}}) \end{aligned} \quad (4.23)$$

with $W_1(0, 0) = 0$, which is positive definite if

$$\begin{cases} \theta\gamma\lambda_2 > 0 \\ \theta(\gamma\lambda_2 - \theta) > 0 \end{cases} \quad \text{and therefore if} \quad \begin{cases} \theta > 0 \\ \gamma\lambda_2 > \theta \end{cases} \quad (4.24)$$

Hence $V(\mathbf{e}, \hat{\mathbf{e}})$ is a suitable Lyapunov function candidate, since $W_1(\mathbf{e}, \hat{\mathbf{e}}) \leq V(\mathbf{e}, \hat{\mathbf{e}}) \leq W_2(\mathbf{e}, \hat{\mathbf{e}})$.

The derivative of (4.20) along the trajectories of (4.15) is given by

$$\dot{V}(\mathbf{e}, \hat{\mathbf{e}}) = -[\theta I_m - A(t)] \bar{\mathbf{e}}^\top \mathcal{J}_T(\hat{\mathbf{e}}, t) G \varepsilon(\hat{\mathbf{e}}) - \gamma \dot{\mathbf{e}}^\top \dot{\mathbf{e}} + \theta \dot{\mathbf{e}}^\top \dot{\mathbf{e}} \quad (4.25)$$

Exploiting inequality (4.18), we obtain

$$\dot{V}(\mathbf{e}, \hat{\mathbf{e}}) \leq -[\theta I_m - A(t)] \bar{\mathbf{e}}^\top \mathcal{J}_T(\hat{\mathbf{e}}, t) G \varepsilon(\hat{\mathbf{e}}) - \left(\gamma - \frac{\theta}{\lambda_2} \right) \dot{\mathbf{e}}^\top \dot{\mathbf{e}} \quad (4.26)$$

and therefore we have $\dot{V}(\mathbf{e}, \hat{\mathbf{e}}) \leq 0$ when (4.24) holds and

$$[\theta I_m - A(t)] > 0 \quad (4.27)$$

By combining conditions (4.22),(4.24) and (4.27) we get

$$\begin{cases} \theta > \alpha_k(t) \\ \gamma \lambda_M > \theta \\ \gamma \lambda_2 > \theta \end{cases} \Rightarrow \begin{cases} \gamma \lambda_M > \theta > \alpha_k(t) \\ \gamma \lambda_2 > \theta > \alpha_k(t) \end{cases} \Rightarrow \begin{cases} \gamma \lambda_M > \max_{t \geq 0} \alpha_k(t) \\ \gamma \lambda_2 > \max_{t \geq 0} \alpha_k(t) \end{cases} \quad \forall k \quad (4.28)$$

If we denote with $\bar{\alpha}_k$ the maximum of the α_k functions, the last expression yields:

$$\gamma > \max \left\{ \frac{\bar{\alpha}_k}{\lambda_M}, \frac{\bar{\alpha}_k}{\lambda_2} \right\} \quad \forall k \quad (4.29)$$

Since $\lambda_M = \lambda_{\max}(L_E)$ by definition and $\lambda_{\max}(L_E) = \lambda_{\max}(L)$ because the communication graph is connected (cfr. Lemma 4, [9]), the aforementioned condition becomes $\gamma > \max \{ \bar{\alpha}_k / \lambda_{\max}(L), \bar{\alpha}_k / \lambda_2(L) \}$. Finally, $\lambda_2(L) < \lambda_{\max}(L)$ implies (4.19). Hence if (4.29) is satisfied, $\dot{V}(\mathbf{e}, \hat{\mathbf{e}})$ is negative semi-definite and this implies that $V(\mathbf{e}, \hat{\mathbf{e}}) \leq V(\mathbf{e}(0), \hat{\mathbf{e}}(0))$ which in turn implies that $\mathbf{e}, \varepsilon(\hat{\mathbf{e}}) \in \mathcal{L}_\infty$, given that $V(\mathbf{e}(0), \hat{\mathbf{e}}(0))$ is bounded. Therefore, if $\hat{\mathbf{e}}(0)$ is chosen within the performance regions (2.5) then $V(\mathbf{e}(0), \hat{\mathbf{e}}(0))$ is bounded, $\varepsilon(\hat{\mathbf{e}}) \in \mathcal{L}_\infty$ and consequently $\hat{\mathbf{e}}(t)$ evolves within the prescribed performance regions $\forall t$. Since $\bar{x} = \bar{\mathbf{e}}$, the relative positions $\bar{x}(t)$ evolve within the prescribed performance bounds (2.2) and we have proved *i*).

Computing now the second derivative of $\dot{V}(\mathbf{e}, \hat{\mathbf{e}})$, we can conclude that it is bounded based on the fact that $\varepsilon(\hat{\mathbf{e}})$ and $\dot{\varepsilon}(\hat{\mathbf{e}})$ are bounded. Boundedness of $\ddot{V}(\mathbf{e}, \hat{\mathbf{e}})$ implies that $\dot{V}(\mathbf{e}, \hat{\mathbf{e}})$ is uniformly continuous and therefore, by applying Barbalat's Lemma, $\dot{V}(\mathbf{e}, \hat{\mathbf{e}}) \rightarrow 0$ as $t \rightarrow \infty$. If the transformation functions T_k are chosen such that $T_k(0) = 0$, then $\dot{V}(\mathbf{e}, \hat{\mathbf{e}}) \rightarrow 0$ implies $\bar{\mathbf{e}} \rightarrow 0$ and $\dot{\bar{\mathbf{e}}} \rightarrow 0$ as $t \rightarrow \infty$. If $\bar{\mathbf{e}} \rightarrow 0$, then $B^\top \mathbf{e} \rightarrow 0$ and therefore $\mathbf{e} \rightarrow \{\eta_1 \mathbb{1}_N, 0\}$. If $\mathbf{e} = 0$, then $x = c_x \mathbb{1}_N$, otherwise if $\mathbf{e} = \eta_1 \mathbb{1}_N$ we have

$$x - c_x \mathbb{1}_N = \eta_1 \mathbb{1}_N \quad \Longrightarrow \quad \mathbb{1}_N^\top x - c_x \mathbb{1}_N^\top \mathbb{1}_N = \eta_1 \mathbb{1}_N^\top \mathbb{1}_N$$

and as a consequence of Lemma 4.1 we obtain

$$\mathbb{1}_N^\top x_0 - c_x \mathbb{1}_N^\top \mathbb{1}_N = \eta_1 \mathbb{1}_N^\top \mathbb{1}_N \quad \Longrightarrow \quad \eta_1 = 0$$

Besides if $\bar{v} \rightarrow 0$ then $B^\top v \rightarrow 0$ and subsequently $v \rightarrow \{\eta_2 \mathbb{1}_N, 0\}$. If $v = \eta_2 \mathbb{1}_N$, using (4.6), we have

$$\mathbb{1}_N^\top v = \eta_2 \mathbb{1}_N^\top \mathbb{1}_N \quad \Longrightarrow \quad \mathbb{1}_N^\top v_0 = \eta_2 \mathbb{1}_N^\top \mathbb{1}_N$$

that under Assumption 4 implies $\eta_2 = 0$. Thus, we have also proved *iii*. \square

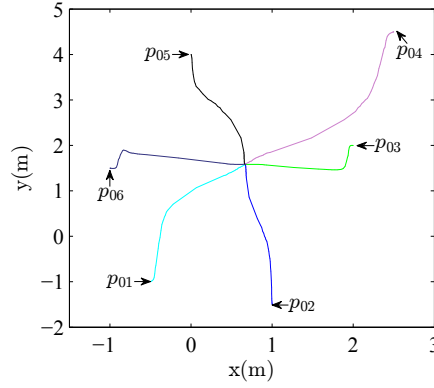


Figure 4.1: Agents trajectories on the $x - y$ plane with PPC2 in case of \mathcal{G}_1 . $\gamma = 390$ and $G = 36I_m$

For details on how the Lyapunov function (4.20) was obtained refer to Appendix C. For the expression of \ddot{V} see Appendix D.

4.4 Simulations

In this section we present the simulations of the proposed controller (PPC2). Similarly to the previous controller we consider $N = 6$ agents moving on a planar surface, starting with velocity equal to zero from the initial positions $p_{01} = [-0.5 \ -1]^\top$, $p_{02} = [1 \ -1.5]^\top$, $p_{03} = [2 \ 2]^\top$, $p_{04} = [2.5 \ 4.5]^\top$, $p_{05} = [0 \ 4]^\top$, $p_{06} = [-1 \ 1.5]^\top$. We also use the performance function

$$\rho(t) = (8 - 10^{-2}) \exp^{-2t} + 10^{-2}$$

and the transformation function (3.20) with $M = 0.1$, which are the same for each pair of neighbouring agents. For this choice of the transformation function condition (4.19) becomes

$$\gamma > \frac{\tau}{\lambda_2(L)} \left(\frac{\rho_0 - \rho_\infty}{\rho_0} \right) \quad (4.30)$$

In this case the minimum allowed value for the damping γ is dependent on the underlying graph of connections and in particular depends on the second smallest eigenvalue of the associated Laplacian matrix. Three topologies are considered, which are the same of Section 3.4 (see Figure 3.1), hence the condition is different in each case:

- spanning tree (\mathcal{G}_1): $\lambda_2(L) = 0.3249$, and then it has to be $\gamma > 6.148$;
- connected graph with one cycle (\mathcal{G}_2): $\lambda_2(L) = 0.6972$, implying $\gamma > 2.865$;
- complete graph (\mathcal{G}_3): $\lambda_2(L) = 6$, and therefore $\gamma > 0.3329$.

By choosing $\gamma = 390$ and $G = 36I_m$ all the other hypotheses of Theorem 4.2 are satisfied and we are guaranteed that the position errors will evolve within the bounds and the agents will reach consensus, with final value $c_\infty = \frac{1}{N} \sum_{i=1}^6 p_{i0} = [0.6667 \quad 1.5833]^\top$.

In Figure 4.1 the trajectories of the agents on the plane are shown, whereas Figure 4.2 shows how the relative positions evolve within the performance bounds.

Observing the velocities' plots (Figures 4.3-4.4) and comparing them with the simulations of the previous controller, we notice that we need a higher value for the gain γ to obtain a comparable behaviour in terms of oscillations of the absolute velocities while approaching the steady state. On the other hand a larger gain induces a smoother evolution for the relative velocities, that is reflected also on the behaviour of the absolute velocities (compare to Figure 3.4 of the previous chapter).

We already pointed out, based on (4.30), that in order to tune the parameter γ it is necessary to know a priori the structure of the communication graph, and that undermines the distributed nature of this type of controller. On the other hand, experimental results show that the value that γ should be considerably larger than the one given from (4.30), independently of underlying topology. Hence the controller can be tuned disregarding the information on $\lambda_2(L)$.

Moreover, observing Figure 4.7, we can notice that the structure of the communication graph does not affect the time required to reach consensus: in fact if the graph is

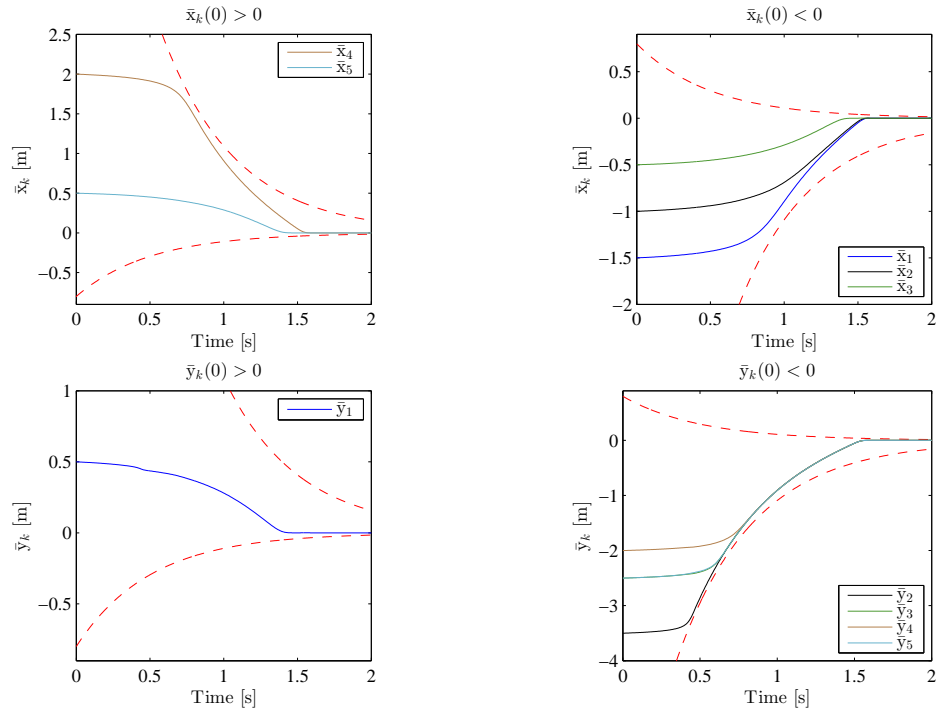


Figure 4.2: Relative positions (solid lines) and performance bounds (dashed lines) in case of \mathcal{G}_1 , with $\gamma = 390$ and $G = 36I_m$.

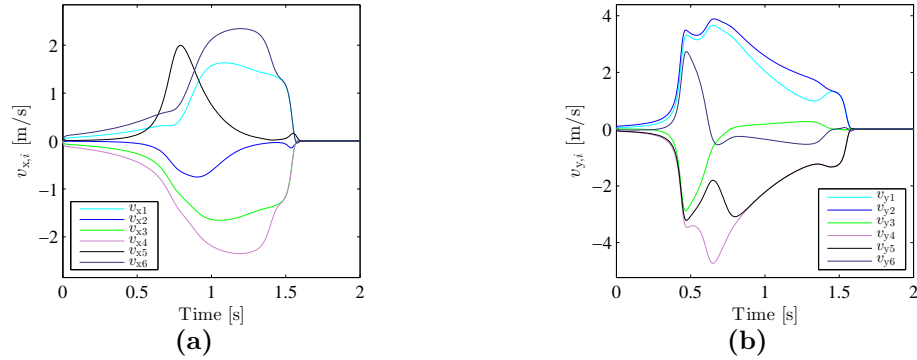


Figure 4.3: Absolute velocities along (a) x coordinate and (b) y coordinate in case of \mathcal{G}_1 , with $\gamma = 390$ and $G = 36I_m$.

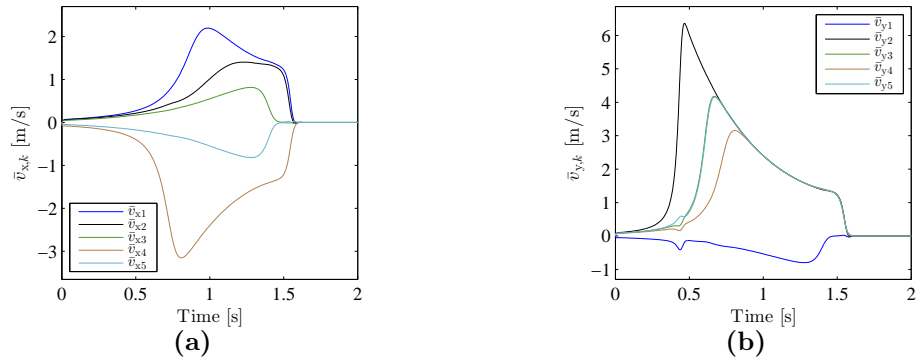


Figure 4.4: Relative velocities along (a) x coordinate and (b) y coordinate in case of \mathcal{G}_1 , with $\gamma = 390$ and $G = 36I_m$.

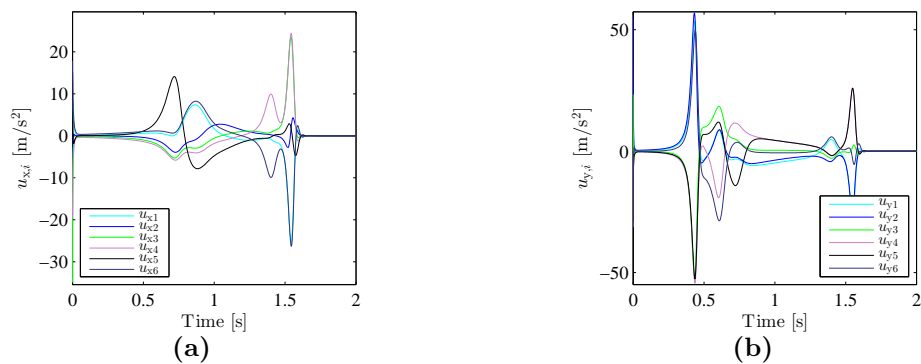


Figure 4.5: Control inputs along (a) x coordinate and (b) y coordinate in case of \mathcal{G}_1 , with $\gamma = 360$ and $G = 36I_m$.

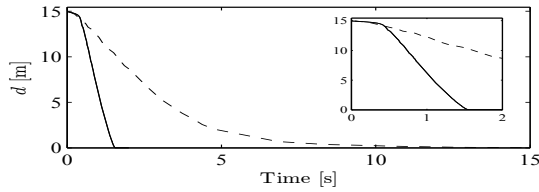


Figure 4.6: Comparison of nonlinear (PPC2, solid line) and linear (dashed line) protocol in case of \mathcal{G}_1 : time evolution of the distance from the centroid.

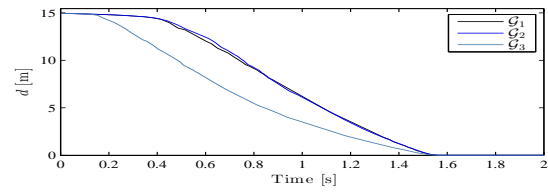


Figure 4.7: Comparison of the performance of PPC2 with different topologies for the connections between agents.

either a spanning tree, connected with a cycle or complete convergence is obtained in approximately the same time. Repeated simulations showed that this behaviour persists while changing the values of γ and G .

As with the previous controller, the nonlinear approach allows to obtain a considerably faster convergence to the consensus value if compared to the linear one, $\dot{\xi} =$

$$\begin{bmatrix} \mathbf{0}_N & I_N \\ -L & -\gamma_L L \end{bmatrix} \xi^2.$$

²Once again the value of the parameter γ_L is chosen in order to guarantee the maximum rate of convergence possible with the considered configuration while avoiding oscillatory behaviours. For this type of second-order linear protocol, the condition ensuring that the eigenvalues of Γ are all real, is given in [8].

Chapter 5

Prescribed transient behaviour for both position errors and combined errors

5.1 Combined error

In this chapter the objective is to constrain the relative positions $\bar{x}(t)$ within the regions (2.5) while, at the same time, imposing some additional bounds to the evolution of a linear combination of the velocity and the position error (addressed as *combined error*). Let us define

$$q_{ij} \triangleq v_{ij} + \kappa_{ij}x_{ij} \quad i \in \mathcal{V} \quad \text{and} \quad j \in \mathcal{N}_i \quad (5.1)$$

with κ_{ij} positive constants, that can alternatively be written as

$$\bar{q}_k \triangleq \bar{v}_k + \bar{\kappa}_k \bar{x}_k \quad (5.2)$$

with $\bar{\kappa}_k \triangleq \kappa_{ij}$, for $k = 1, 2, \dots, m$. We want to constrain \bar{q}_k within the following bounds:

$$-M_{k,\bar{q}}\rho_{k,\bar{q}}(t) < \bar{q}_k(t) < \rho_{k,\bar{q}}(t) \quad \text{if} \quad \bar{q}_k(0) \geq 0 \quad (5.3a)$$

$$-\rho_{k,\bar{q}}(t) < \bar{q}_k(t) < M_{k,\bar{q}}\rho_{k,\bar{q}}(t) \quad \text{if} \quad \bar{q}_k(0) < 0 \quad (5.3b)$$

with $M_{k,\bar{q}}$ overshoot index and $\rho_{k,\bar{q}}(t)$ performance function of \bar{q}_k , for $k = 1, 2, \dots, m$. By denoting with $\hat{q}_k(t) = \frac{\bar{q}_k(t)}{\rho_k(t)}$ the modified combined errors we can define the corresponding

prescribed performance regions:

$$D_{\hat{q}_k} \triangleq \{\hat{q}_k(t) : \hat{q}_k(t) \in (-M_{k,\bar{q}}, 1)\} \quad \text{if} \quad \bar{q}_k(0) \geq 0 \quad (5.4a)$$

$$D_{\hat{q}_k} \triangleq \{\hat{q}_k(t) : \hat{q}_k(t) \in (-1, M_{k,\bar{q}})\} \quad \text{if} \quad \bar{q}_k(0) < 0 \quad (5.4b)$$

We also define the following quantities:

- ▷ \bar{q} is the stack vector of all combined errors \bar{q}_k for $k = 1, \dots, m$. Therefore the following identity holds

$$\bar{q} = \bar{v} + K\bar{x} \quad (5.5)$$

with $K = \bar{\kappa}_k I_m$.

- ▷ $\varepsilon(\hat{q})$ is the stack vector of all modified combined errors $\varepsilon_k(\hat{q}_k)$ for $k = 1, \dots, m$. The domain of the vector function $\varepsilon(\hat{q})$ is the Cartesian product of all the open sets $D_{\hat{q}_k}$, $k = 1, \dots, m$, i.e.

$$D_{\hat{q}} = D_{\hat{q}_1} \times D_{\hat{q}_2} \times \dots \times D_{\hat{q}_m}$$

We want to establish a relation similar to (2.21) and (2.22) between the vectors $q = \dot{x} + \Gamma x$ and \bar{q} , i.e. we require

$$\bar{q} = B^\top q \quad (5.6)$$

where $\Gamma = \gamma I_N$. Writing (5.6) as $\bar{q} = B^\top v + B^\top \Gamma x$ and considering that in (5.5) we already defined \bar{q} as $\bar{q} = \bar{v} + KB^\top x$, it is clear that a condition on the matrices K and Γ is implied:

$$B^\top \Gamma = KB^\top \quad (5.7)$$

Consequently $\bar{\kappa}_k = \bar{\kappa} \forall k$ and $\gamma = \bar{\kappa}$.

5.2 Proposed controller

In order to achieve the new control objective, we propose the following nonlinear distributed controller:

$$u_i = - \sum_{j \in \mathcal{N}_i} [\mathcal{J}_{T_{ij}}(\hat{q}_{ij}, t) \varepsilon_{ij}(\hat{q}_{ij}) + g_{ij} \mathcal{J}_{T_{ij}}(\hat{x}_{ij}, t) \varepsilon_{ij}(\hat{x}_{ij})] - \gamma v_i \quad i \in \mathcal{V} \quad (5.8)$$

where g_{ij} are positive constant gains and all the other terms have already been defined. Let $G_{\bar{x}} \in \mathbb{R}^{m \times m}$ be a diagonal, positive definite, gain matrix with diagonal elements g_{ij} .

The system (2.19), with the control (5.8) can be now written in vector form as

$$\begin{aligned}\dot{x} &= v \\ \dot{v} &= -B\mathcal{J}_T(\hat{q}, t)\varepsilon(\hat{q}) - B\mathcal{J}_T(\hat{x}, t)G\varepsilon(\hat{x}) - \gamma v\end{aligned}\quad (5.9)$$

or equivalently

$$\ddot{x} = -B\mathcal{J}_T(\hat{q}, t)\varepsilon(\hat{q}) - B\mathcal{J}_T(\hat{x}, t)G\varepsilon(\hat{x}) - \gamma v \quad (5.10)$$

Considering $q = \dot{x} + \Gamma x$, we can also write (5.10) as a first order system:

$$\dot{q} = -B\mathcal{J}_T(\hat{q}, t)\varepsilon(\hat{q}) - B\mathcal{J}_T(\hat{x}, t)G\varepsilon(\hat{x}) \quad (5.11)$$

Such a form will be useful when studying the stability of the closed loop system.

5.3 Time evolution of the centroid

As in the previous cases we try to obtain an analytical expression describing how the means of positions and velocities of the agents vary during time.

We multiply both sides of the second equation of (5.9) by the vector $\mathbb{1}_N^\top$, obtaining

$$\begin{aligned}\mathbb{1}_N^\top \dot{v} &= -\mathbb{1}_N^\top B\mathcal{J}_T(\hat{x}, t)G\varepsilon(\hat{x}) - \mathbb{1}_N^\top B\mathcal{J}_T(\hat{q}, t)\varepsilon(\hat{q}) - \gamma \mathbb{1}_N^\top v \\ \frac{d}{dt} \left(\sum_{i=1}^N v_i \right) &= -\gamma \sum_{i=1}^N v_i\end{aligned}\quad (5.12)$$

that is the same result we have for the first presented controller, cfr. (3.4). This renders the investigation of the centroid evolution identical to what has already been done in Section 3.2. Therefore, the equation describing the evolution of the sum of absolute velocities is given by

$$\frac{1}{N} \sum_{i=1}^N v_i(t) = \left(\frac{1}{N} \sum_{i=1}^N v_i(0) \right) e^{-\gamma t} \quad (5.13)$$

which will asymptotically converge to 0.

Similarly, the centroid will evolve as in (3.8), i.e.

$$c(t) = \frac{1}{N} \mathbb{1}_N^\top x_0 - \frac{1}{\gamma} \left(\frac{1}{N} \mathbb{1}_N^\top v_0 \right) (e^{-\gamma t} - 1) \quad (5.14)$$

asymptotically converging to, see (3.9),

$$c_\infty = \frac{1}{N} \mathbb{1}_N^\top x_0 + \frac{1}{\gamma} \left(\frac{1}{N} \mathbb{1}_N^\top v_0 \right) \quad (5.15)$$

5.4 Stability analysis

Let $\rho_{\bar{x},k}(t)$, $M_{\bar{x},k}$ and $T_{\bar{x},k}$ be respectively the performance functions, the overshoot index and the transformation functions associated to the position errors \bar{x}_k for $k = 1, 2, \dots, m$. Let also $T_{\bar{q},k}$ denote the transformation functions applied to the modified errors \hat{q}_k . The conditions that ensure stability of the closed loop system (5.10) are given in the following theorem:

Theorem 5.1. *Consider the prescribed performance agreement protocol (5.8) applied to the double integrator dynamics (2.19), under Assumptions 1, 2, 3 and with performance functions $\rho_{\bar{x},k}(t)$ having bounded derivative $\forall t \geq 0$ and transformation functions s.t. $T_{\bar{x},k}(0) = 0$ and $T_{\bar{q},k}(0) = 0 \forall k$. Assume also that $\bar{x}(0)$ is within the performance bounds (2.2) and that γ is chosen such that*

$$\gamma > \max_{t \geq 0} \alpha_{\bar{x},k}(t) \quad (5.16)$$

and $\bar{q}_k(0) = \bar{v}_k(0) + \gamma \bar{x}_k(0)$ is within the performance bounds (5.3) for all k .

Then:

- i) the position error $\bar{x}(t)$ evolves within the performance bounds $\forall t \geq 0$ and asymptotically converges to zero,
- ii) the combined error $\bar{q}(t)$ evolves within the performance bounds $\forall t \geq 0$ and asymptotically converges to zero. \diamond

Proof. In order to prove the theorem, we first simplify the notation by indicating $\varepsilon(\hat{q})$ with $\varepsilon_{\hat{q}}$, $\varepsilon(\hat{x})$ with $\varepsilon_{\hat{x}}$, $\mathcal{J}_T(\hat{q}, t)$ with $\mathcal{J}_{T_{\hat{q}}}$ and $\mathcal{J}_T(\hat{x}, t)$ with $\mathcal{J}_{T_{\hat{x}}}$.

The proof consists of three parts: a) proof of the boundedness of the term $\varepsilon_{\hat{x}}$, b) proof of the boundedness of the term $\varepsilon_{\hat{q}}$, c) proof of the asymptotic stability of the equilibrium.

a) Consider the positive definite potential function

$$V_1(q, \hat{x}) = \frac{1}{2} q^\top q + \frac{1}{2} \varepsilon_{\hat{x}}^\top G \varepsilon_{\hat{x}} \quad (5.17)$$

and its derivative along the trajectories of (5.10)

$$\begin{aligned} \dot{V}_1(q, \hat{x}) &= q^\top \dot{q} + \varepsilon_{\hat{x}}^\top G \dot{\varepsilon}_{\hat{x}} \\ \dot{V}_1(\bar{q}, \hat{x}) &= -\bar{q}^\top \mathcal{J}_{T_{\hat{q}}} \varepsilon_{\hat{q}} - [\gamma I_m - A(t)] \bar{x}^\top \mathcal{J}_{T_{\hat{x}}} G \varepsilon_{\hat{x}} \end{aligned} \quad (5.18)$$

which is negative semi-definite if (5.16) holds $\forall k$ (similar to the proof of Theorem 3.1). Since $\dot{V}_1(q, \bar{x})$ is negative semi-definite $V_1(q, \bar{x}) \leq V_1(q(0), \bar{x}(0))$ which in turn implies

that $q, \varepsilon_{\hat{x}} \in \mathcal{L}_\infty$, given that $V_1(q, \hat{x}(0))$ is bounded. Therefore, if $\bar{x}(0)$ is chosen within the performance regions (2.5) then $V_1(q(0), \hat{x}(0))$ is bounded and hence $\varepsilon_{\hat{x}} \in \mathcal{L}_\infty$. Consequently $\hat{x}(t)$ evolves within the prescribed performance regions $\forall t \geq 0$. Furthermore $\varepsilon(\hat{x})$ is bounded and this implies also that the jacobian $\mathcal{J}_T(\hat{x}, t)$ is bounded. We have then proved the first part of *i*).

b) Having proved the boundedness of the term prescribing the position errors, we can define $d(t) = B\mathcal{J}_{T_{\hat{x}}}\varepsilon_{\hat{x}} \in \mathcal{L}_\infty$ and write the system (5.11) in the form

$$\dot{q} + B\mathcal{J}_{T_{\hat{q}}}\varepsilon_{\hat{q}} = d(t) \quad \text{or equivalently} \quad \dot{\bar{q}} + B^\top B\mathcal{J}_{T_{\hat{q}}}\varepsilon_{\hat{q}} = B^\top d(t) \quad (5.19)$$

as a first order system evolving under the effect of a bounded disturbance.

For this part of the proof, let θ being an arbitrary positive constant and consider the following potential function

$$V_2(\varepsilon_{\hat{q}}, q) = \frac{1}{2}\varepsilon_{\hat{q}}^\top \varepsilon_{\hat{q}} + \frac{\theta}{2}q^\top q \quad (5.20)$$

and its derivative along the trajectories of system (5.19)

$$\dot{V}_2(\varepsilon_{\hat{q}}, q) = \varepsilon_{\hat{q}}^\top \dot{\varepsilon}_{\hat{q}} + \theta q^\top \dot{q} \quad (5.21)$$

Taking into account

$$\begin{aligned} \dot{\varepsilon}_{\hat{q}} &= \mathcal{J}_{T_{\hat{q}}}[\dot{\bar{q}} + A(t)\bar{q}] \\ &= -\mathcal{J}_{T_{\hat{q}}}B^\top B\mathcal{J}_{T_{\hat{q}}}\varepsilon_{\hat{q}} + \mathcal{J}_{T_{\hat{q}}}B^\top d(t) + \mathcal{J}_{T_{\hat{q}}}A(t)\bar{q} \end{aligned} \quad (5.22)$$

and substituting (5.22) and (5.11) into (5.21), we obtain

$$\begin{aligned} \dot{V}_2(\varepsilon_{\hat{q}}, q) &= -\varepsilon_{\hat{q}}^\top \mathcal{J}_{T_{\hat{q}}}B^\top B\mathcal{J}_{T_{\hat{q}}}\varepsilon_{\hat{q}} + \varepsilon_{\hat{q}}^\top \mathcal{J}_{T_{\hat{q}}}B^\top d(t) - \varepsilon_{\hat{q}}^\top \mathcal{J}_{T_{\hat{q}}}\dot{P}(t)\hat{q} \\ &\quad - \theta \bar{q}^\top \mathcal{J}_{T_{\hat{q}}}\varepsilon_{\hat{q}} + \theta q^\top d(t) \end{aligned} \quad (5.23)$$

Substituting $\hat{q} = P(t)^{-1}B^\top q$, with $P(t)$ $m \times m$ diagonal matrix defined in (2.12), and considering that the edge Laplacian $B^\top B$ of a connected graph is a positive semi-definite matrix, the following inequality stands:

$$-\varepsilon_{\hat{q}}^\top \mathcal{J}_{T_{\hat{q}}}\dot{P}(t)\hat{q} - \theta \bar{q}^\top \mathcal{J}_{T_{\hat{q}}}\varepsilon_{\hat{q}} \leq -\hat{q}^\top [\theta I_m - A(t)] \frac{\partial \varepsilon_{\hat{q}}}{\partial \hat{q}} \varepsilon_{\hat{q}} \quad (5.24)$$

The matrix $A(t)$ can be simply bounded from above, i.e. $\sup_t(|A(t)|) < \bar{\alpha}$, with some constant $\bar{\alpha}$. By setting $\bar{\mu} := \theta - \bar{\alpha}$ we can bound from above the term on the right of

(5.24) with

$$-\hat{q}^\top [\theta I_m - A(t)] \frac{\partial \varepsilon_{\hat{q}}}{\partial \hat{q}} \varepsilon_{\hat{q}} \leq -\bar{\mu} \hat{q}^\top \frac{\partial \varepsilon_{\hat{q}}}{\partial \hat{q}} \varepsilon_{\hat{q}} \quad (5.25)$$

Consider now the first two terms on the right side of (5.23). We have the following inequalities:

$$-\varepsilon_{\hat{q}}^\top \mathcal{J}_{T_{\hat{q}}} B^\top d(t) \leq \zeta_1 \|B \mathcal{J}_{T_{\hat{q}}} \varepsilon_{\hat{q}}\|^2 + \frac{1}{4\zeta_1} \|d(t)\|^2 \quad (5.26)$$

$$-\varepsilon_{\hat{q}}^\top \mathcal{J}_{T_{\hat{q}}} B^\top B \mathcal{J}_{T_{\hat{q}}} \varepsilon_{\hat{q}} \leq -\|B \mathcal{J}_{T_{\hat{q}}} \varepsilon_{\hat{q}}\|^2 \quad (5.27)$$

Putting (5.26) and (5.27) together we obtain

$$-\varepsilon_{\hat{q}}^\top \mathcal{J}_{T_{\hat{q}}} B^\top B \mathcal{J}_{T_{\hat{q}}} \varepsilon_{\hat{q}} - \varepsilon_{\hat{q}}^\top \mathcal{J}_{T_{\hat{q}}} B^\top d(t) \leq -(1 - \zeta_1) \|B \mathcal{J}_{T_{\hat{q}}} \varepsilon_{\hat{q}}\|^2 + \frac{1}{4\zeta_1} \|d(t)\|^2 \quad (5.28)$$

for some appropriately chosen constants $\zeta_1 < 1$, whereas for the remaining term of the same equation, we can write

$$q^\top d(t) \leq \zeta_2 \|q\|^2 + \frac{1}{4\zeta_2} \|d(t)\|^2 \quad (5.29)$$

for some constant ζ_2 . Considering inequalities (5.25), (5.26), (5.29) and also (2.16) we can bound $\dot{V}_2(\hat{q}, q)$ with

$$\dot{V}_2(\varepsilon_{\hat{q}}, q) \leq -\lambda V_2(\varepsilon_{\hat{q}}, q) + \varphi(t) \quad (5.30)$$

with λ appropriately chosen constant and $\varphi(t)$ bounded term depending on q and $d(t)$ that have already been proved to be bounded in part a). For a complete proof of the inequality refer to Appendix E. By applying Theorem 4.18 of [24] (see Appendix F), we can conclude that $\varepsilon_{\hat{q}}$ and, consequently, $\mathcal{J}_{T_{\hat{q}}}$ are bounded and we have proved the first part of *ii*).

c) Let us recall the potential function (5.17) that we used in part a) and its first derivative along the system's trajectories

$$\dot{V}_1(\bar{q}, \hat{x}) = -\bar{q}^\top \mathcal{J}_{T_{\bar{q}}} \varepsilon_{\hat{q}} - [\gamma I_m - A(t)] \bar{x}^\top \mathcal{J}_{T_{\bar{x}}} G \varepsilon_{\hat{x}}$$

Calculating the second derivative $\ddot{V}_1(\bar{q}, \bar{x})$, we can find that it is bounded based on boundedness of $\varepsilon_{\hat{q}}$, $\varepsilon_{\hat{x}}$ and $\dot{\varepsilon}_{\hat{q}}$, $\dot{\varepsilon}_{\hat{x}}$. This implies that $\dot{V}_1(\bar{q}, \bar{x})$ is uniformly continuous and we can apply Barbalat's Lemma to conclude that, since $T_{\bar{x},k}(0) = 0$ and $T_{\bar{q},k}(0) = 0$, $\bar{q}(t) \rightarrow 0$ and $\bar{x}(t) \rightarrow 0$, completing the proof of both *i*) and *ii*). \square

The only thing remained is to verify if the agents' absolute positions converge to the system's centroid. Along the lines of Corollary 3.2, we can state the following complementary result:

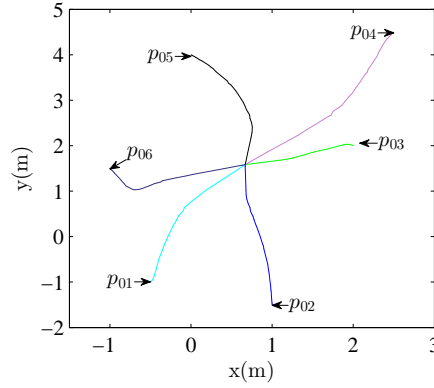


Figure 5.1: Agents trajectories on the $x-y$ plane with PPC3 in case of \mathcal{G}_1 , with $G = 2I_m$, $\gamma = 3$.

Corollary 5.2. Consider the prescribed performance agreement protocol (5.8) applied to the double integrator dynamics (2.19) with all the assumptions of Theorem 5.1. The agreement protocol ensures convergence of the agents' absolute positions to the centroid.

◇

Proof. The proof is identical to the one of Corollary 3.2.

□

5.5 Simulations

For the simulations we considered 6 agents moving on a plane, starting with initial positions $p_{01} = [-0.5 \ -1]^\top$, $p_{02} = [1 \ -1.5]^\top$, $p_{03} = [2 \ 2]^\top$, $p_{04} = [2.5 \ 4.5]^\top$, $p_{05} = [0 \ 4]^\top$, $p_{06} = [-1 \ 1.5]^\top$ and zero initial velocity. We used an exponentially decreasing performance functions for both the relative positions and \bar{q} :

$$\rho(t) = (8 - 10^{-2}) \exp^{-2t} + 10^{-2}$$

$$\rho_{\bar{q}}(t) = (20 - 10^{-2}) \exp^{-3t} + 10^{-2}$$

Note that $\rho(t)$ is the same of Section 3.4 and $\gamma > 1.9975$. Note also that in this case the agents do not need to have a priori knowledge of the structure of the underlying communication graph to tune this parameter. The modified errors $\hat{q}_{x,k}$, $\hat{q}_{y,k}$ ¹, \hat{x}_k and \hat{y}_k are transformed with the logarithmic function (3.20), which is the same for each k , and the overshoot indices are chosen as $M = 0.1$ and $M_{\bar{q}} = 0.1$. By further choosing the matrix gain as $G = 2I_m$ and the damping as $\gamma = 3$, and by considering a spanning tree communication graph (\mathcal{G}_1), agreement is guaranteed and the controlled variables

¹Let $\bar{q}_{x,k} = \bar{v}_x + \gamma \bar{x}_k$ and $\bar{q}_{y,k} = \bar{v}_y + \gamma \bar{y}_k$ denote the modified errors along the x and y coordinate respectively. $\hat{q}_{x,k}$ and $\hat{q}_{y,k}$ are the correspondent modified errors.

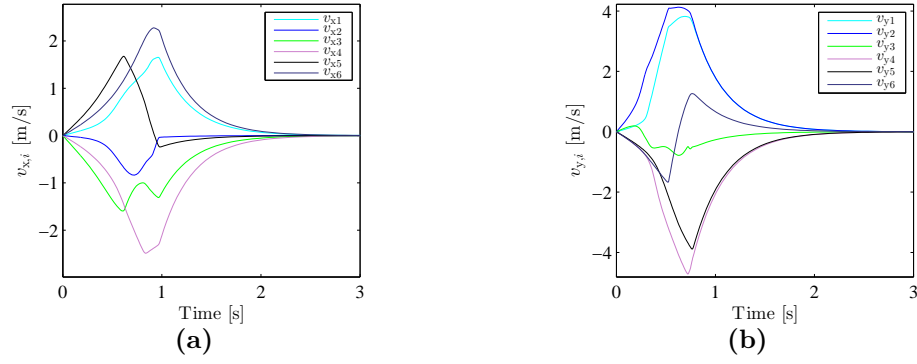


Figure 5.2: Absolute velocities along (a) x coordinate and (b) y coordinate in case of \mathcal{G}_1 , with $\gamma = 3$ and $G = 2I_m$.

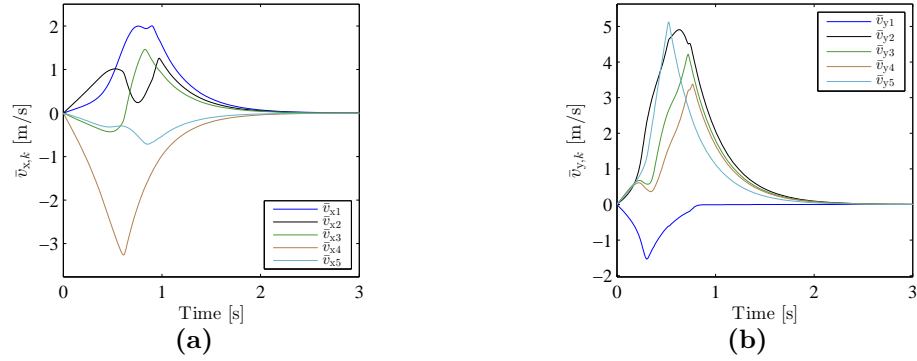


Figure 5.3: Relative velocities along (a) x coordinate and (b) y coordinate in case of \mathcal{G}_1 , with $\gamma = 3$ and $G = 2I_m$.

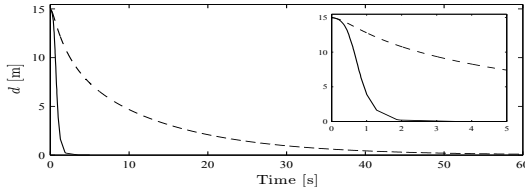


Figure 5.4: Comparison between PPC3 (solid line), with $\gamma = 3$ and $G = 2I_m$, and the linear protocol (dashed line). Case of \mathcal{G}_1 .

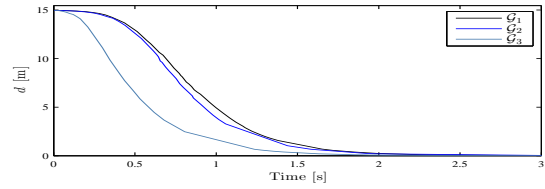


Figure 5.5: Comparison of the performance of PPC3 for different graph topologies. Distance from the centroid. $\gamma = 3$, $G = 2I_m$.

evolve within the bounds (see Theorem 5.1). Moreover, Corollary 5.2 ensures that the final consensus value coincides with the centroid. Simulation results for this settings are shown in Figures 5.1-5.6. With the introduction of the performance bounds on the combined error, oscillations are avoided for values of γ which are considerably lower than needed with the previous controllers. Yet, if compared to PPC1 and PPC2, we are able to obtain a smoother evolution for the velocity response. Note also that, differently from PPC1 and PPC2, even a small gain G allows to obtain a low value for the control inputs. Repeated simulations have also shown that a value of $\tau_{\bar{q}}$ larger than τ reduces, and in some cases prevents, oscillations in the evolution of $\bar{q}_x(t)$ and $\bar{q}_y(t)$ and yields a smooth behaviour. Finally, we also considered the cases when the communication

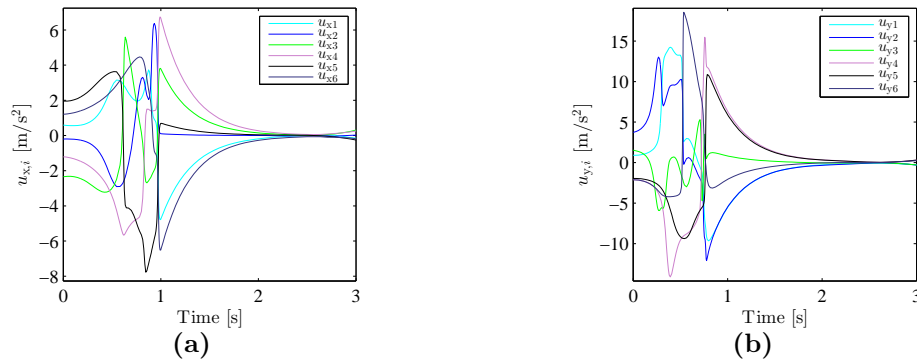


Figure 5.6: Control inputs along (a) x coordinate and (b) y coordinate in case of \mathcal{G}_1 , with $\gamma = 3$ and $G = 2I_m$.

graph is connected with a cycle (\mathcal{G}_3) and complete (\mathcal{G}_3). Figure 5.5 shows that with \mathcal{G}_2 and \mathcal{G}_3 the rate of convergence increases due to the presence of cycles: this is evident in the case of a complete graph. The same behaviour is typical of the linear agreement protocols, since cycles influence the value of the second smallest eigenvalue of L . In Figure 5.4 is shown the comparison with the linear protocol (the same of Section 3.4): once again, the bounds on the evolution of \bar{x} (and \bar{y}) guaranteeing the independence of the graph's topology allow to reach a considerably faster rate of convergence.

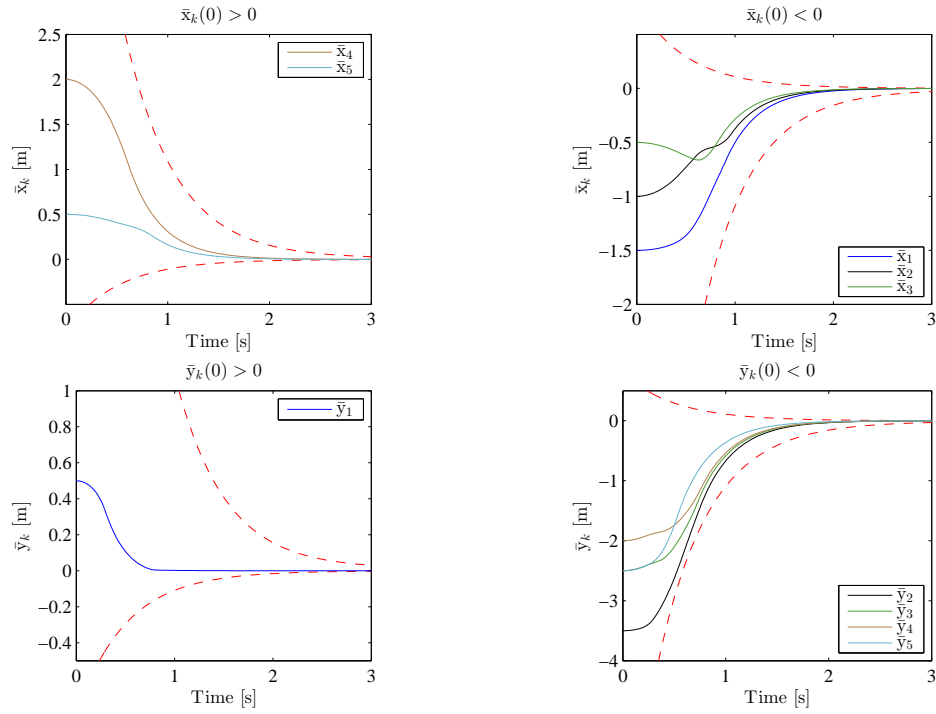


Figure 5.7: Relative positions (solid lines) and performance bounds (dashed lines) in case of \mathcal{G}_1 , with $\gamma = 3$ and $G = 2I_m$.

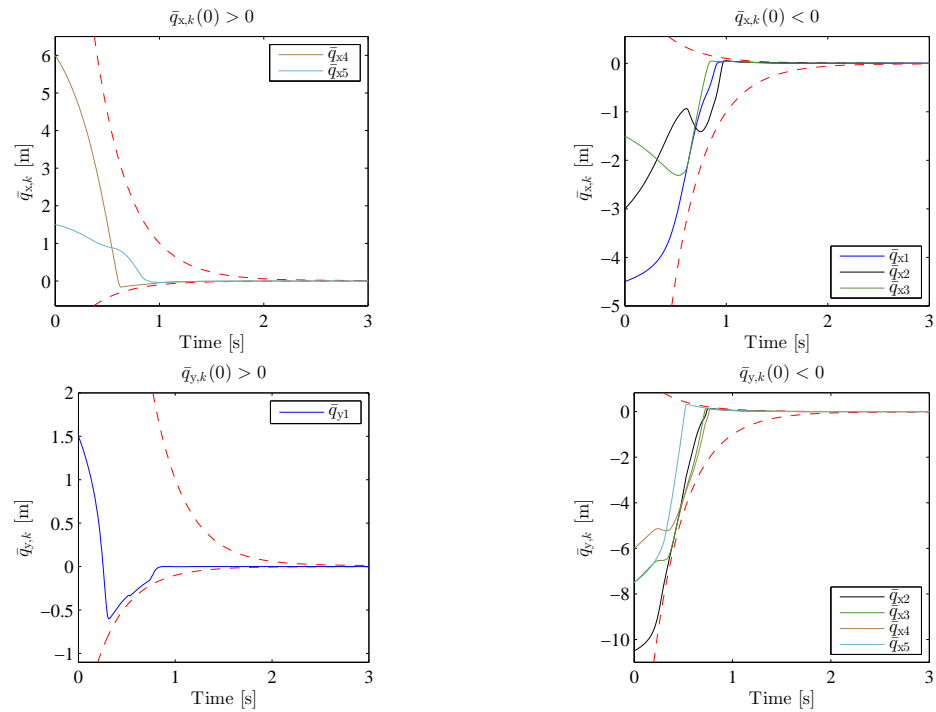


Figure 5.8: Combined error (solid lines) and performance bounds (dashed lines) in case of \mathcal{G}_1 , with $\gamma = 3$ and $G = 2I_m$.

Chapter 6

Conclusions and future work

In this thesis we proposed three different nonlinear distributed controllers able to reach consensus while guaranteeing predefined specifications such as overshoot and maximum rate of convergence in the edge's space. We considered a group of agents described by a double-integrator model exchanging information about their current position and velocity. By applying prescribed performance control we were able to restrict the evolution of the position errors between neighbouring agents within a priori imposed time-variant bounds, obtaining a rate of convergence which is independent of the topology of the network. This overcomes a typical problem of the linear consensus algorithms, in which the convergence is governed by the algebraic connectivity of the communication graph.

First we analysed the case in which time-dependent bounds are imposed only on the evolution of the relative positions between communicating agents. The proposed controller consisted of two terms: a nonlinear term depending on the position errors and a damping term depending on the absolute velocities. We also proposed another controller considering the relative velocities instead. In both cases the stability analysis yielded a condition for the damping gain in order to guarantee that the trajectories converge to the equilibrium that coincides with the agents' centroid. Moreover we proved that when the sum of initial velocities is equal to zero, time-invariance of the centroid is guaranteed provided that the neighbouring agents share the same prescribed performance function, overshoot index and transformation function. Simulations of both closed loop systems validated the theoretical findings while demonstrating that by appropriately designing the performance function, the nonlinear protocol can achieve a faster convergence compared to the linear one. It was also observed that a large value for the damping parameter can smoothen the velocity response. Furthermore, by modifying the constant gains of the prescribed performance term, we can affect the distance between the error and the bounds during the evolution.

In the last part of the work, we considered additional time-dependent bounds on the combined error. We proposed a protocol not only guaranteeing average consensus but also ensuring that both relative positions and combined error evolve within the pre-defined regions. Also in this case the condition for stability involved the value of the damping gain and the agents positions converge to the centroid. Nonetheless, we proved the invariance of the centroid during time when the sum of initial velocities is zero. Simulations showed that with such a controller the response of the velocities is considerably smoother than in the previous cases and oscillations are avoided for small values of the damping.

Future work includes further investigation the last controller in order to be able to introduce some constraints on the the relative velocities and the extension of the results to multi agent systems with more complex dynamics, such as nonholonomic robots.

Appendix A

Derivation of the potential function (3.12) in Theorem 3.1

We can derive a suitable potential positive definite function to prove Theorem 3.1 analysing the following inner products (we omit the argument \hat{x} and t from $\mathcal{J}_T(\hat{x}, t)$ and $\varepsilon(\hat{x})$):

$$\theta x^\top \ddot{x} = -\theta x^\top B \mathcal{J}_T G \varepsilon - \theta \gamma x^\top \dot{x}$$

$$\frac{d}{dt} (\theta x^\top \dot{x}) - \theta \dot{x}^\top \dot{x} = -\theta x^\top B \mathcal{J}_T G \varepsilon - \theta \gamma x^\top \dot{x} \quad (\text{A.1})$$

$$\dot{x}^\top \ddot{x} = -\dot{x}^\top B \mathcal{J}_T G \varepsilon - \gamma \dot{x}^\top \dot{x}$$

$$\frac{d}{dt} \left(\frac{1}{2} \dot{x}^\top \dot{x} \right) = -\dot{x}^\top B \mathcal{J}_T G \varepsilon - \gamma \dot{x}^\top \dot{x} \quad (\text{A.2})$$

Adding side by side (A.1) and (A.2) we obtain

$$\begin{aligned} \dot{x}^\top \ddot{x} + \theta x^\top \ddot{x} &= -\dot{x}^\top B \mathcal{J}_T G \varepsilon - \gamma \dot{x}^\top \dot{x} - \theta x^\top B G \mathcal{J}_T \varepsilon - \theta \gamma x^\top \dot{x} \\ \frac{d}{dt} (\theta x^\top \dot{x}) + \frac{d}{dt} \left(\frac{1}{2} \dot{x}^\top \dot{x} \right) + \theta \gamma x^\top \dot{x} &= -\theta \bar{x}^\top \mathcal{J}_T G \varepsilon - (\gamma - \theta) \dot{x}^\top \dot{x} - \dot{x}^\top \mathcal{J}_T G \varepsilon \\ \frac{d}{dt} (\theta x^\top \dot{x}) + \frac{d}{dt} \left(\frac{1}{2} \dot{x}^\top \dot{x} \right) + \frac{d}{dt} \left(\frac{\theta \gamma}{2} x^\top x \right) &= -\theta \bar{x}^\top \mathcal{J}_T G \varepsilon - (\gamma - \theta) \dot{x}^\top \dot{x} - \dot{x}^\top \mathcal{J}_T G \varepsilon \end{aligned}$$

By adding and subtracting on the right side the quantity $A(t) \bar{x}^\top \mathcal{J}_T G \varepsilon$, the previous equation becomes

$$\begin{aligned} \frac{d}{dt} (\theta x^\top \dot{x}) + \frac{d}{dt} \left(\frac{1}{2} \dot{x}^\top \dot{x} \right) + \frac{d}{dt} \left(\frac{\theta \gamma}{2} x^\top x \right) &= -\theta \bar{x}^\top \mathcal{J}_T G \varepsilon - (\gamma - \theta) \dot{x}^\top \dot{x} \\ &\quad - [\dot{x} + A(t) \bar{x}]^\top \mathcal{J}_T G \varepsilon \\ &\quad + A(t) \bar{x}^\top \mathcal{J}_T G \varepsilon \end{aligned}$$

$$\begin{aligned} \frac{d}{dt} (\theta x^\top \dot{x}) + \frac{d}{dt} \left(\frac{1}{2} \dot{x}^\top \dot{x} \right) + \frac{d}{dt} \left(\frac{\theta \gamma}{2} x^\top x \right) &= -\theta \bar{x}^\top \mathcal{J}_T G \varepsilon - (\gamma - \theta) \dot{x}^\top \dot{x} \\ &\quad - \dot{\varepsilon}^\top \mathcal{J}_T^{-1} \mathcal{J}_T G \varepsilon + A(t) \bar{x}^\top \mathcal{J}_T G \varepsilon \end{aligned}$$

$$\begin{aligned} \frac{d}{dt} (\theta x^\top \dot{x}) + \frac{d}{dt} \left(\frac{1}{2} \dot{x}^\top \dot{x} \right) + \frac{d}{dt} \left(\frac{\theta\gamma}{2} x^\top x \right) + \frac{d}{dt} \left(\frac{1}{2} \varepsilon^\top G \varepsilon \right) = \\ - [\theta I_m - A(t)] \bar{x}^\top \mathcal{J}_T G \varepsilon - (\gamma - \theta) \dot{x}^\top \dot{x} \end{aligned}$$

and the left side of this equation is the derivative of Lyapunov function (3.12) of Theorem 3.1.

Appendix B

Second derivative of the potential function (3.12) in Theorem 3.1

Let us briefly recall the expression (3.14) of the first derivative of Lyapunov function (3.12)

$$\dot{V}(\xi, \hat{x}) = -[\theta I_m - A(t)] \bar{x}^T \mathcal{J}_T(\hat{x}, t) G \varepsilon(\hat{x}) - (\gamma - \theta) \dot{x}^T \dot{x} \quad (\text{B.1})$$

Let us then define $\nu \triangleq (\gamma - \theta)$ and clarify that from now on we will omit the argument \hat{x} and t from $\mathcal{J}_T(\hat{x}, t)$ and $\varepsilon(\hat{x})$.

Differentiating (B.1) with respect to time, we obtain

$$\begin{aligned} \ddot{V}(\xi, \hat{x}) &= -\frac{d}{dt}([\theta I_m - A(t)] \bar{x}^T \mathcal{J}_T G \varepsilon) - \nu \frac{d}{dt}(\dot{x}^T \dot{x}) \\ &= -\frac{d}{dt}([\theta I_m - A(t)]) \bar{x}^T \mathcal{J}_T G \varepsilon - [\theta I_m - A(t)] \frac{d}{dt}(\bar{x}^T \mathcal{J}_T G \varepsilon) - 2\nu \dot{x}^T \ddot{x} \\ &= \dot{A}(t) \bar{x}^T \mathcal{J}_T G \varepsilon - [\theta I_m - A(t)] (\bar{x}^T \mathcal{J}_T G \dot{\varepsilon} + \dot{\bar{x}}^T \mathcal{J}_T G \varepsilon) + \\ &\quad - [\theta I_m - A(t)] \left(\bar{x}^T \frac{d}{dt}(\mathcal{J}_T) G \varepsilon \right) + 2\nu \dot{\bar{x}}^T \mathcal{J}_T G \varepsilon + 2\nu \gamma \dot{x}^T \dot{x} \\ &= \dot{A}(t) \bar{x}^T \mathcal{J}_T G \varepsilon + 2\nu \dot{\bar{x}}^T \mathcal{J}_T G \varepsilon + 2\nu \gamma \dot{x}^T \dot{x} - [\theta I_m - A(t)] \bar{x}^T \mathcal{J}_T G \dot{\varepsilon} + \\ &\quad - [\theta I_m - A(t)] \left(\dot{\bar{x}}^T \mathcal{J}_T G \varepsilon + \bar{x}^T \left[P^{-1}(t) \frac{d}{dt} \left(\frac{\partial T}{\partial \hat{x}} \right) + A(t) \mathcal{J}_T \right] G \varepsilon \right) \\ &= \dot{A}(t) \bar{x}^T \mathcal{J}_T G \varepsilon + 2\nu \dot{\bar{x}}^T \mathcal{J}_T G \varepsilon + 2\nu \gamma \dot{x}^T \dot{x} - [\theta I_m - A(t)] \bar{x}^T \mathcal{J}_T G \dot{\varepsilon} + \\ &\quad - [\theta I_m - A(t)] [\dot{\bar{x}}^T \mathcal{J}_T G \varepsilon + A(t) \bar{x}^T \mathcal{J}_T G \varepsilon] + \\ &\quad - [\theta I_m - A(t)] \bar{x}^T \left[P^{-1}(t) \frac{d}{dt} \left(\frac{\partial T}{\partial \hat{x}} \right) \right] G \varepsilon \end{aligned} \quad (\text{B.2})$$

where we have denoted with $\frac{\partial T}{\partial \hat{x}}$ the $m \times m$ diagonal matrix with entries $\frac{\partial T_k}{\partial \hat{x}_k}$, with $\dot{A}(t)$ the $m \times m$ diagonal matrix with entries $\dot{\alpha}_k(t)$ and with $P^{-1}(t)$ the $m \times m$ diagonal matrix with entries $\frac{1}{\rho_k(t)}$.

To infer the boundedness of $\ddot{V}(\xi, \hat{x})$, a further investigation of the terms $\mathcal{J}_T(\hat{x}, t)$ and $\frac{d}{dt} \left(\frac{\partial T}{\partial \hat{x}} \right)$ is required.

Recalling (2.9) and (2.11), it is clear that boundedness of \mathcal{J}_T depends on the terms $\frac{\partial T_k}{\partial \hat{x}_k}$,

whose analytical expression is:

- for $\bar{x}_k(0) > 0$

$$\begin{aligned} \frac{\partial T_k}{\partial \hat{x}_k} &= \frac{\partial}{\partial \hat{x}_k} \left(\ln \left(\frac{M_k + \hat{x}_k}{M_k(1 - \hat{x}_k)} \right) \right) \\ &= \frac{M_k(1 - \hat{x}_k)}{M_k + \hat{x}_k} \frac{M_k(1 - \hat{x}_k) + (M_k + \hat{x}_k)M_k}{M_k^2(1 - \hat{x}_k)^2} \\ &= \frac{M_k + 1}{(M_k + \hat{x}_k)(1 - \hat{x}_k)} \end{aligned}$$
- for $\bar{x}_k(0) < 0$

$$\begin{aligned} \frac{\partial T_k}{\partial \hat{x}_k} &= \frac{\partial}{\partial \hat{x}_k} \left(\ln \left(\frac{M_k(1 + \hat{x}_k)}{M_k - \hat{x}_k} \right) \right) \\ &= \frac{M_k - \hat{x}_k}{M_k(1 + \hat{x}_k)} \frac{M_k(M_k - \hat{x}_k) + (1 + \hat{x}_k)M_k}{(M_k - \hat{x}_k)^2} \\ &= \frac{M_k + 1}{(M_k - \hat{x}_k)(1 + \hat{x}_k)} \end{aligned}$$

where we have considered T defined as in (2.17).

Summarizing, the analytical expression for the partial derivative of the transformation function is

$$\frac{\partial T_k}{\partial \hat{x}_k} = \begin{cases} \frac{M_k + 1}{(M_k + \hat{x}_k)(1 - \hat{x}_k)} & \text{if } \bar{x}_k(0) > 0 \\ 0 & \text{if } \bar{x}_k(0) = 0 \\ \frac{M_k + 1}{(M_k - \hat{x}_k)(1 + \hat{x}_k)} & \text{if } \bar{x}_k(0) < 0 \end{cases} \quad (\text{B.3})$$

The derivative with respect to time of (B.3) is

$$\frac{d}{dt} \left(\frac{\partial T_k}{\partial \hat{x}_k} \right) = \frac{\partial^2 T_k}{\partial \hat{x}_k^2} \dot{\hat{x}}_k = \frac{1}{\rho_k(t)} \frac{\partial^2 T_k}{\partial \hat{x}_k^2} [\dot{\hat{x}}_k - \rho_k(t) \hat{x}_k]$$

and it is bounded if \bar{x}_k and $\frac{\partial^2 T_k}{\partial \hat{x}_k^2}$ are. In the following we calculate the second order partial derivative, which is:

- for $\bar{x}_k(0) > 0$

$$\begin{aligned} \frac{\partial^2 T_k}{\partial \hat{x}_k^2} &= \frac{\partial}{\partial \hat{x}_k} \left(\frac{M_k + 1}{(M_k + \hat{x}_k)(1 - \hat{x}_k)} \right) \\ &= (M_k + 1) \frac{-\frac{d}{dt} ((M_k + \hat{x}_k)(1 - \hat{x}_k))}{(M_k + \hat{x}_k)^2(1 - \hat{x}_k)^2} \end{aligned}$$

$$\begin{aligned}
&= -(M_k + 1) \frac{[-(M_k + \hat{x}_k) + (1 - \hat{x}_k)]}{(M_k + \hat{x}_k)^2 (1 - \hat{x}_k)^2} \\
&= (M_k + 1) \frac{2\hat{x}_k + M_k - 1}{(M_k + \hat{x}_k)^2 (1 - \hat{x}_k)^2} \\
\bullet \text{ for } \bar{x}_k(0) < 0 \quad \frac{\partial^2 T_k}{\partial \hat{x}_k^2} &= \frac{\partial}{\partial \hat{x}_k} \left(\frac{M_k + 1}{(M_k - \hat{x}_k)(1 + \hat{x}_k)} \right) \\
&= -(M_k + 1) \frac{(M_k - \hat{x}_k) - (1 + \hat{x}_k)}{(M_k - \hat{x}_k)^2 (1 + \hat{x}_k)^2} \\
&= (M_k + 1) \frac{2\hat{x}_k + 1 - M_k}{(M_k - \hat{x}_k)^2 (1 + \hat{x}_k)^2}
\end{aligned}$$

and then, summarizing

$$\frac{\partial^2 T_k}{\partial \hat{x}_k^2} = \begin{cases} \frac{(M_k+1)(2\hat{x}_k+M_k-1)}{(M_k+\hat{x}_k)^2(1-\hat{x}_k)^2} & \text{if } \bar{x}_k(0) > 0 \\ 0 & \text{if } \bar{x}_k(0) = 0 \\ \frac{(M_k+1)(2\hat{x}_k+1-M_k)}{(M_k-\hat{x}_k)^2(1+\hat{x}_k)^2} & \text{if } \bar{x}_k(0) < 0 \end{cases} \quad (\text{B.4})$$

Based on (B.2), (B.3) and (B.4), the boundedness of $\ddot{V}(\xi, \hat{x})$ depends on

- ▷ \bar{x} and $\dot{\hat{x}}$, which are bounded based on $V(\xi, \hat{x}) \leq V(\xi(0), \hat{x}(0))$
- ▷ $\varepsilon(\hat{x})$, which is bounded since \bar{x} is bounded
- ▷ $\dot{\varepsilon}(\hat{x})$, which is bounded since $\varepsilon(\hat{x})$ is bounded
- ▷ $\mathcal{J}_T(\hat{x}, t)$, which is bounded based on the fact that \bar{x} is
- ▷ $\frac{d}{dt} \left(\frac{\partial T}{\partial \hat{x}} \right)$, which boundedness is implied by the boundedness of \bar{x}

we can conclude that $\ddot{V}(\xi, \hat{x})$ is bounded.

Appendix C

Derivation of the Lyapunov function (4.20) in Theorem 4.2

We can obtain a suitable Lyapunov function to prove Theorem 4.2 by taking the following inner product (we omit the argument \hat{e} and t from $\mathcal{J}_T(\hat{e}, t)$ and $\varepsilon(\hat{e})$):

$$\begin{aligned} \theta e^T \ddot{e} &= -\theta e^T B \mathcal{J}_T G \varepsilon - \theta \gamma e^T B B^T \dot{e} \\ \frac{d}{dt} (\theta e^T \dot{e}) - \theta \dot{e}^T \dot{e} &= -\theta e^T B \mathcal{J}_T G \varepsilon - \theta \gamma \bar{e}^T \dot{e} \\ \frac{d}{dt} (\theta e^T \dot{e}) + \frac{d}{dt} \left(\frac{\theta \gamma}{2} \bar{e}^T \bar{e} \right) &= -\theta e^T B \mathcal{J}_T G \varepsilon + \theta \dot{e}^T \dot{e} \end{aligned} \quad (C.1)$$

Then, if we consider the inner product

$$\dot{e}^T \ddot{e} = -\dot{e}^T B \mathcal{J}_T G \varepsilon - \gamma \dot{e}^T B B^T \dot{e}$$

further adding and subtracting on the right side the quantity $A(t) \bar{e}^T \mathcal{J}_T G \varepsilon$, we obtain

$$\begin{aligned} \frac{d}{dt} \left(\frac{1}{2} \dot{e}^T \dot{e} \right) &= -[\dot{e} + A(t) \bar{e}]^T \mathcal{J}_T G \varepsilon - \gamma \dot{e}^T \dot{e} + A(t) \bar{e}^T \mathcal{J}_T G \varepsilon \\ \frac{d}{dt} \left(\frac{1}{2} \dot{e}^T \dot{e} \right) + \dot{e}^T G \varepsilon &= A(t) \bar{e}^T \mathcal{J}_T G \varepsilon - \gamma \dot{e}^T \dot{e} \\ \frac{d}{dt} \left(\frac{1}{2} \dot{e}^T \dot{e} \right) + \frac{d}{dt} \left(\frac{1}{2} \varepsilon^T G \varepsilon \right) &= A(t) \bar{e}^T \mathcal{J}_T G \varepsilon - \gamma \dot{e}^T \dot{e} \end{aligned} \quad (C.2)$$

Adding side by side (C.1) and (C.2), we finally get

$$\frac{d}{dt} \left(\frac{\theta \gamma}{2} \bar{e}^T \bar{e} \right) + \frac{d}{dt} (\theta e^T \dot{e}) + \frac{d}{dt} \left(\frac{1}{2} \dot{e}^T \dot{e} \right) + \frac{d}{dt} \left(\frac{1}{2} \varepsilon^T G \varepsilon \right) = -[\theta I_m - A(t)] \bar{e}^T \mathcal{J}_T G \varepsilon - \gamma \dot{e}^T \dot{e} + \theta \dot{e}^T \dot{e}$$

and the term on the left side is the derivative of Lyapunov function (4.20) of Theorem 4.2.

Appendix D

Second derivative of the Lyapunov function (4.20) in Theorem 4.2

Let us recall the expression (4.25) of the first derivative of Lyapunov function (4.20)

$$\dot{V}(\mathbf{e}, \hat{\mathbf{e}}) = -[\theta I_m - A(t)] \bar{\mathbf{e}}^T \mathcal{J}_T(\hat{\mathbf{e}}, t) G \varepsilon(\hat{\mathbf{e}}) - \gamma \dot{\mathbf{e}}^T \dot{\mathbf{e}} + \theta \dot{\mathbf{e}}^T \dot{\mathbf{e}} \quad (\text{D.1})$$

Derivating (D.1) with respect to time, we find:

$$\begin{aligned} \ddot{V}(\mathbf{e}, \hat{\mathbf{e}}) &= -\frac{d}{dt} ([\theta I_m - A(t)] \bar{\mathbf{e}}^T \mathcal{J}_T G \varepsilon) - \gamma \frac{d}{dt} (\dot{\mathbf{e}}^T \dot{\mathbf{e}}) + \theta \frac{d}{dt} (\dot{\mathbf{e}}^T \dot{\mathbf{e}}) \\ &= -\frac{d}{dt} ([\theta I_m - A(t)] \bar{\mathbf{e}}^T \mathcal{J}_T G \varepsilon) - [\theta I_m - A(t)] \frac{d}{dt} (\bar{\mathbf{e}}^T \mathcal{J}_T G \varepsilon) + \\ &\quad - 2\gamma \dot{\mathbf{e}}^T \ddot{\mathbf{e}} + 2\theta \dot{\mathbf{e}}^T \ddot{\mathbf{e}} \\ &= \dot{A}(t) \bar{\mathbf{e}}^T \mathcal{J}_T G \varepsilon - [\theta I_m - A(t)] (\bar{\mathbf{e}}^T \mathcal{J}_T G \dot{\varepsilon} + \dot{\bar{\mathbf{e}}}^T \mathcal{J}_T G \varepsilon) + \\ &\quad - [\theta I_m - A(t)] \bar{\mathbf{e}}^T \frac{d}{dt} (\mathcal{J}_T) G \varepsilon - 2\gamma \dot{\mathbf{e}}^T \ddot{\mathbf{e}} + 2\theta \dot{\mathbf{e}}^T \ddot{\mathbf{e}} \\ &= \dot{A}(t) \bar{\mathbf{e}}^T \mathcal{J}_T G \varepsilon - [\theta I_m - A(t)] (\bar{\mathbf{e}}^T \mathcal{J}_T G \dot{\varepsilon} + \dot{\bar{\mathbf{e}}}^T \mathcal{J}_T G \varepsilon) + \\ &\quad - [\theta I_m - A(t)] \left(\bar{\mathbf{e}}^T \left[P^{-1}(t) \frac{d}{dt} \left(\frac{\partial T}{\partial \hat{\mathbf{e}}} \right) + A(t) \mathcal{J}_T \right] G \varepsilon \right) \\ &\quad - 2\gamma \dot{\mathbf{e}}^T \ddot{\mathbf{e}} + 2\theta \dot{\mathbf{e}}^T \ddot{\mathbf{e}} \end{aligned}$$

Based on the analytical expressions for the terms $\mathcal{J}_T(\hat{\mathbf{e}}, t)$ and $\frac{d}{dt} \left(\frac{\partial T}{\partial \hat{\mathbf{e}}} \right)$ that have been already given in Appendix B, we can state that the upper bound on $\ddot{V}(\mathbf{e}, \hat{\mathbf{e}})$ depends on

- ▷ $\bar{\mathbf{e}}$ and $\dot{\bar{\mathbf{e}}}$, which are bounded based on $V(\mathbf{e}, \hat{\mathbf{e}}) \leq V(\mathbf{e}(0), \hat{\mathbf{e}}(0))$
- ▷ $\varepsilon(\hat{\mathbf{e}})$, which is bounded since $\bar{\mathbf{e}}$ is bounded
- ▷ $\mathcal{J}_T(\hat{\mathbf{e}}, t)$, which is bounded based on the fact that $\bar{\mathbf{e}}$ is
- ▷ $\ddot{\mathbf{e}}$ and $\ddot{\bar{\mathbf{e}}}$, which are bounded due to boundedness of all previous terms
- ▷ $\dot{\varepsilon}(\hat{\mathbf{e}})$, which is bounded since $\varepsilon(\hat{\mathbf{e}})$ is bounded
- ▷ $\frac{d}{dt} \left(\frac{\partial T}{\partial \hat{\mathbf{e}}} \right)$, whose boundedness is due to the boundedness of $\bar{\mathbf{e}}$

and therefore $\ddot{V}(\mathbf{e}, \hat{\mathbf{e}})$ is bounded.

Appendix E

Proof of inequality (5.30)

Let us recall (5.23):

$$\begin{aligned} \dot{V}_2(\hat{q}, q) &= -\varepsilon_{\hat{q}}^\top \mathcal{J}_{T_{\hat{q}}} B^\top B \mathcal{J}_{T_{\hat{q}}} \varepsilon_{\hat{q}} - \varepsilon_{\hat{q}}^\top \mathcal{J}_{T_{\hat{q}}} \dot{P}(t) \hat{q} + \varepsilon_{\hat{q}}^\top \mathcal{J}_{T_{\hat{q}}} B^\top d(t) \\ &\quad - \bar{q}^\top \mathcal{J}_{T_{\hat{q}}} \varepsilon_{\hat{q}} + q^\top d(t) \end{aligned} \quad (\text{E.1})$$

Considering inequalities (5.25), (5.26) and also (5.27), we can bound $\dot{V}_2(\hat{q}, q)$ with

$$\begin{aligned} \dot{V}_2(\hat{q}, q) &\leq -(1 - \zeta_1) \|B \mathcal{J}_{T_{\hat{q}}} \varepsilon_{\hat{q}}\|^2 - \bar{\mu} \hat{q}^\top \frac{\partial \varepsilon_{\hat{q}}}{\partial \hat{q}} \varepsilon_{\hat{q}} + \zeta_2 \|q\|^2 + \left(\frac{1}{4\zeta_1} + \frac{1}{4\zeta_2} \right) \|d(t)\|^2 \\ \dot{V}_2(\hat{q}, q) &\leq -\bar{\mu} \hat{q}^\top \frac{\partial \varepsilon_{\hat{q}}}{\partial \hat{q}} \varepsilon_{\hat{q}} + \zeta_2 \|q\|^2 + \left(\frac{1}{4\zeta_1} + \frac{1}{4\zeta_2} \right) \|d(t)\|^2 \end{aligned} \quad (\text{E.2})$$

Adding and subtracting the quantity $\mu_2 \|q\|^2$, with μ_2 being an appropriately chosen constant, (E.2) becomes

$$\dot{V}_2(\hat{q}, q) \leq -\bar{\mu} \hat{q}^\top \frac{\partial \varepsilon_{\hat{q}}}{\partial \hat{q}} \varepsilon_{\hat{q}} - \mu_2 \|q\|^2 + \varphi(t) \quad (\text{E.3})$$

where $\varphi(t) = (\mu_2 + \zeta_2) \|q\|^2 + \left(\frac{1}{4\zeta_1} + \frac{1}{4\zeta_2} \right) \|d(t)\|^2$ is a bounded term given the boundedness of q and $d(t)$.

From inequality (2.16), we obtain that

$$-\bar{\mu} \hat{q}^\top \frac{\partial \varepsilon_{\hat{q}}}{\partial \hat{q}} \varepsilon_{\hat{q}} \leq \bar{\mu} \mu_1 \|\varepsilon_{\hat{q}}\|^2$$

where μ_1 chosen constant, hence imposing $\lambda = 2\mu_2 = 2\bar{\mu}\mu_1$ (E.3) becomes

$$\dot{V}_2(\hat{q}, q) \leq -\lambda V_2(\varepsilon_{\hat{q}}, q) + \varphi(t) \quad (\text{E.4})$$

Appendix F

Proof of boundedness of $\varepsilon(\hat{q})$ in Theorem 5.1

For the sake of completeness we recall Theorem 4.18 of [24]:

Theorem (4.18, Khalil). *Let $D \subset \mathbb{R}^n$ be a domain that contains the origin and $V : [0, \infty) \times D \rightarrow \mathbb{R}$ be a continuously differentiable function such that*

$$\alpha_1(\|x\|) \leq V(t, x) \leq \alpha_2(\|x\|)$$

$$\frac{\partial V}{\partial t} + \frac{\partial V}{\partial x} f(t, x) \leq -W_3(x), \quad \forall \|x\| \geq \mu > 0$$

$\forall t \geq 0$ and $\forall x \in D$, where α_1 and α_2 are class \mathcal{K} functions and $W_3(x)$ is continuous positive definite function. Take $r > 0$ such that $B_r \subset D$ and suppose that

$$\mu < \alpha^{-1}(\alpha_1(r))$$

Then, there exists a class \mathcal{KL} function β and for every initial state $x(t_0)$, satisfying $\|x(t_0)\| \leq \alpha_2^{-1}(\alpha_1(r))$, there is $T > 0$ (dependent on $x(t_0)$ and μ) such that the solution of $\dot{x} = f(t, x)$ satisfies

$$\|x(t)\| \leq \beta(\|x(t_0)\|, t - t_0), \quad \forall t_0 \leq t \leq t_0 + T \quad (\text{F.1})$$

$$\|x(t)\| \leq \alpha_2^{-1}(\alpha_1(r)), \quad \forall t_0 \geq t_0 + T \quad (\text{F.2})$$

Moreover, if $D = \mathbb{R}^n$ and α_1 belongs to class \mathcal{K}_∞ then (F.1) and (F.2) hold for any initial state $x(t_0)$, with no restriction on how large μ is. \diamond

In part b) of the proof of Theorem 5.1 we obtained the inequality

$$\dot{V}_2(\varepsilon_{\hat{q}}, q) \leq -\lambda V_2(\varepsilon_{\hat{q}}, q) + \varphi(t) \quad (\text{F.3})$$

and denoting $\bar{\varphi} = \sup_t \varphi(t)$, (F.3) becomes

$$\dot{V}_2(\varepsilon_{\hat{q}}, q) \leq -\lambda V_2(\varepsilon_{\hat{q}}, q) + \bar{\varphi} \quad (\text{F.4})$$

Let us define $\mathbf{q} = \begin{bmatrix} \varepsilon_{\hat{q}} \\ q \end{bmatrix}$ and the set $\Omega_\sigma = \{\mathbf{q} \in \mathbb{R}^2 : V(\mathbf{q}) < \frac{\bar{\varphi}}{\lambda}\}$ s.t. $\dot{V}_2(\mathbf{q})$ is negative outside of Ω_σ .

Since, by definition, $V_2(\mathbf{q}) = \frac{1}{2}\|\mathbf{q}\|^2$, Ω_σ is the set of all $\mathbf{q} \in D_{\hat{q}}$ such that

$$\|\mathbf{q}\| \geq \sqrt{\frac{2\bar{\varphi}}{\lambda}}$$

Therefore, choosing for example

$$\alpha_1(\|\mathbf{q}\|) = \frac{1}{4}\|\mathbf{q}\|^2, \quad \alpha_2(\|\mathbf{q}\|) = \|\mathbf{q}\|^2 \quad \text{and} \quad \mu = \sqrt{2\bar{\varphi}/\lambda}$$

the previously stated theorem guarantees the uniformly ultimately boundedness of the state \mathbf{q} .

Appendix G

Condition (3.11) for an exponentially decreasing performance function

Consider a performance function of the form (2.3). The condition (3.11), i.e. $\gamma > \max_{t \geq 0} \alpha_k(t)$, for convergence of the prescribed performance controller (3.1) consequently gives a relation between the time constants τ and the velocities' gain γ . The derivative of $\rho(t)$ is given by $\dot{\rho}(t) = -\tau(\rho_0 - \rho_\infty)e^{-\tau t}$, therefore

$$\alpha(t) = \frac{-\tau(\rho_0 - \rho_\infty)e^{-\tau t}}{(\rho_0 - \rho_\infty)e^{-\tau t} + \rho_\infty}$$

Calculating the derivative of the function $\alpha(t)$, we get:

$$\dot{\alpha}(t) = -\frac{\tau^2(\rho_0 - \rho_\infty)e^{-\tau t}\rho_\infty}{[(\rho_0 - \rho_\infty)e^{-\tau t} + \rho_\infty]^2} < 0 \quad \forall t \geq 0$$

implying that $\alpha(t)$ is monotonically decreasing. Hence the maximum value is given by

$$\max_{t \geq 0} \alpha(t) = \alpha(0) = \tau \left(\frac{\rho_0 - \rho_\infty}{\rho_0} \right)$$

Appendix H

Proof of inequalities (4.17) and (4.18)

In this appendix an alternative way to prove inequalities (4.17) and (4.18) is presented.

As in [9], let us assume that the singular value decomposition of the incidence matrix B of the communication graph is $B = U\Sigma V^T$ with $U \in \mathbb{R}^{N \times N}$ composed by the normalized eigenvectors of $BB^T = L$ and $V \in \mathbb{R}^{m \times m}$ composed by the normalized eigenvectors of $B^T B = L_E$. U and V are orthogonal matrices, implying $UU^T = U^T U = I$ and the same for V . The matrix $\Sigma \in \mathbb{R}^{N \times m}$ has the structure

$$\Sigma = \begin{bmatrix} \sigma_N & 0 & \cdots & 0 \\ 0 & \sigma_{N-1} & \cdots & 0 \\ \vdots & \vdots & \ddots & \vdots \\ 0 & 0 & \ddots & \sigma_2 \\ \hline 0 & 0 & 0 & 0 \end{bmatrix}$$

with $\sigma_N \geq \sigma_{N-1} \geq \cdots \geq \sigma_2$ singular values. We know that $\sigma_i^2 = \lambda_i(L)$ for $i = 2, 3, \dots, N$ are the first $N - 1$ eigenvalues of the Laplacian matrix; moreover we know that the remaining eigenvalue of L is $\lambda_1(L) = 0$.

Using the SVD of B , the Laplacian matrix can be decomposed as

$$BB^T = (U\Sigma V^T)(U\Sigma V^T)^T = U\Sigma V^T V \Sigma^T U^T = U\Sigma \Sigma^T U^T = USU^T$$

with

$$S = \Sigma \Sigma^T = \begin{bmatrix} \lambda_N & 0 & \cdots & 0 & | & 0 \\ 0 & \lambda_{N-1} & \cdots & 0 & | & 0 \\ \vdots & \vdots & \ddots & \vdots & | & \vdots \\ 0 & 0 & \ddots & \lambda_2 & | & 0 \\ \hline 0 & 0 & 0 & 0 & | & 0 \end{bmatrix} \in \mathbb{R}^{N \times N}$$

Given that the matrices U and V are not unique, we can always choose $U = [u_N, u_{N-1}, \dots, u_1]$ s.t. u_i is the normalised eigenvector relative to the eigenvalue λ_i . In particular, since the eigenvector corresponding to $\lambda_1 = 0$ is $\mathbb{1}_N$, we can choose U s.t. $u_1 = \frac{1}{\sqrt{N}} \mathbb{1}_N$.

Consider now the quadratic form $e^T BB^T e$ and the vectors e s.t. $e \perp u_1$. Using the decomposition obtained before, it can be written

$$\begin{aligned}
 e^T BB^T e &= e^T U S U^T e = \sum_{i=1}^N \lambda_i |(U^T e)_i|^2 \\
 &= \sum_{i=2}^N \lambda_i |(U^T e)_i|^2 \\
 &\geq \lambda_2 \sum_{i=2}^N |(U^T e)_i|^2 \\
 &= \lambda_2 \sum_{i=1}^N |(U^T e)_i|^2 \\
 &= \lambda_2 e^T U U^T e \\
 &= \lambda_2 e^T e
 \end{aligned}$$

Summarizing, we obtained that

$$e^T BB^T e \geq \lambda_2 e^T e$$

for all e such that $e \perp \mathbb{1}_N$, completing the proof of (4.17). The proof of (4.18) is equivalent.

References

- [1] C. H. Caicedo-Nunez and M. Zefran, “Consensus-based rendezvous,” in *Control Applications, 2008. CCA 2008. IEEE International Conference on*. IEEE, 2008, pp. 1031–1036.
- [2] H. G. Tanner, A. Jadbabaie, and G. J. Pappas, “Flocking in fixed and switching networks,” *IEEE Transaction on Automatic Control*, vol. 52, no. 5, pp. 863–868, May 2007.
- [3] S. Lisenmaier, “Event-triggered control of multi-agent systems with double-integrator dynamics: Application to vehicle platooning and flocking algorithms,” Master’s Thesis, School of Electrical Engineering, KTH Royal Institute of Technology, October 2014.
- [4] R. Olfati-Saber and R. M. Murray, “Consensus protocols for networks of dynamic agents,” in *Proceedings of the 2003 American Control Conference*, vol. 2, June 4–6 2003, pp. 951–956.
- [5] R. Olfati-Saber, J. A. Fax, and R. M. Murray, “Consensus and cooperation in networked multi-agent systems,” in *Proceedings of the IEEE*, vol. 95, no. 1, January 2007, pp. 215–233.
- [6] D. Zelazo, A. Rahmani, and M. Mesbahi, “Agreement via the edge laplacian,” in *46th IEEE Conference on Decision and Control*, New Orleans, LA, USA, December 12–14, 2007, pp. 2309–2314.
- [7] G. Xie and L. Wang, “Consensus control for a class of network of dynamic agents: Fixed topology,” in *Proceedings of the 44th IEEE Conference on Decision and Control, and European Control Conference*, Seville, Spain, December 12–15, 2006, pp. 96–101.
- [8] W. Ren and E. Atkins, “Distributed multi-vehicle coordinated control via local information exchange,” *International Journal of Robust and Nonlinear Control*, vol. 17, no. 10–11, pp. 1002–1033, July 2007.
- [9] G. Meng and D. V. Dimarogonas, “Quantized cooperative control using relative states measurements,” in *50th IEEE Conference on Decision and Control and European Control Conference (CDC-ECC)*, Orlando, FL, USA, December 12–15, 2011.

-
- [10] R. Olfati-Saber and R. M. Murray, "Consensus problems in networks of agents with switching topology and time-delays," *IEEE Transaction on Automatic Control*, vol. 49, no. 9, pp. 1520–1533, September 2004.
- [11] M. Ji and M. Egerstedt, "Distributed coordination control of multiagent systems while preserving connectedness," *IEEE Transaction on Robotics*, vol. 23, no. 4, pp. 693–703, August 2007.
- [12] D. Q. Mayne, J. B. Rawlings, C. V. Rao, and P. O. Scokaert, "Constrained model predictive control: Stability and optimality," *Automatica*, vol. 36, no. 6, pp. 789–814, 2000.
- [13] K. P. Tee, S. S. Ge, and E. H. Tay, "Barrier lyapunov functions for the control of output-constrained nonlinear systems," *Automatica*, vol. 45, no. 4, pp. 918–927, 2009.
- [14] C. P. Bechlioulis and G. A. Rovithakis, "Robust partial-state feedback prescribed performance control of cascade systems with unknown nonlinearities," *Automatic Control, IEEE Transactions on*, vol. 56, no. 9, pp. 2224–2230, 2011.
- [15] A. Ilchmann, E. P. Ryan, and S. Trenn, "Tracking control: Performance funnels and prescribed transient behaviour," *Systems & Control Letters*, vol. 54, no. 7, pp. 655–670, 2005.
- [16] C. P. Bechlioulis and G. A. Rovithakis, "Adaptive control with guaranteed transient and steady state tracking error bounds for strict feedback systems," *Automatica*, vol. 45, no. 2, pp. 532–538, February 2009.
- [17] —, "Robust adaptive control of feedback linearizable mimo nonlinear systems with prescribed performance," *IEEE Transactions on Automatic Control*, vol. 53, no. 9, pp. 2090–2099, October 2008.
- [18] Y. Karayiannidis and Z. Doulgeri, "Model-free robot joint position regulation and tracking with prescribed performance guarantees," *Robotics and Autonomous Systems*, vol. 60, no. 2, pp. 214–226, 2012.
- [19] M. Zambelli, Y. Karayiannidis, and D. V. Dimarogonas, "Posture regulation for unicycle-like robots with prescribed performance guarantees," *IET Control Theory & Applications*, 2014, to appear.
- [20] Y. Karayianidis, D. V. Dimarogonas, and D. Kragic, "Multi-average consensus control with prescribed performance guarantees," in *51st IEEE Conference on Decision and Control*, Maui, Hawaii, December 2012.

-
- [21] C. Godsil and G. Royle, *Algebraic graph theory*, ser. Graduate Texts in Mathematics. New York: Springer-Verlag, 2001, vol. 207.
- [22] R. A. Horn and C. R. Johnson, *Matrix Analysis*. New York, NY, USA: Cambridge University Press, 1986.
- [23] M. Mesbahi and M. Egerstedt, *Graph Theoretic Methods in Multiagent Networks*. Princeton University Press, 2010.
- [24] H. Khalil, *Nonlinear Systems*, 3rd ed. Prentice Hall, 2002.